1 **Supporting material for Sullivan et al. Diversity and carbon storage across the tropical forest**
2 **biome**

3 Martin J. P. Sullivan[a,1,*], Joey Talbot[a, 1], Simon L. Lewis[a,b, 1], Oliver L. Phillips[a, 1], Lan Qie[a], Serge K.

4 Begne[a,c], Jerôme Chave[d], Aida Cuni Sanchez[b], Wannes Hubau[a], Gabriela Lopez-Gonzalez[a], Lera

5 Miles[e], Abel Monteagudo-Mendoza[f,g], Bonaventure Sonké[c], Terry Sunderland[h,i], Hans ter Steege[j,k],

6 Lee J. T. White[l,m,n], Kofi Affum-Baffoe[o], Shin-ichiro Aiba[p], Everton C. Almeida[q], Edmar Almeida de

7 Oliveira[kkk], Patricia Alvarez-Loayza[fff], Esteban Álvarez Dávila[kk], Ana Andrade[r], Luiz E.O.C. Aragão[s],

8 Peter Ashton[t], Gerardo A. Aymard C.[u], Timothy R. Baker[a], Michael Balinga[v], Lindsay F. Banin[w],

9 Christopher Baraloto[x], Jean-Francois Bastin[y,z], Nicholas Berry[aa], Jan Bogaert[bb], Damien Bonal[cc], Frans

10 Bongers[dd], Roel Brienen[a], , José Luís C. Camargo[ee], Carlos Cerón[ff], Victor Chama Moscoso[g], Eric

11 Chezeaux[gg], Connie J. Clark[hh], Álvaro Cogollo Pacheco [ppp], James A Comiskey[ii], Fernando Cornejo

12 Valverde[jjjj], Eurídice N. Honorio Coronado[jj], Greta Dargie[a], Stuart J. Davies[ll], Charles De Canniere[mm],

13 Marie Noel Djuikouo K.[nn], Jean-Louis Doucet[oo], Terry L. Erwin[pp], Javier Silva Espejo[g], Corneille

14 E.N. Ewango[qq,rr], Sophie Fauset[a,ss], Ted R. Feldpausch[s], Rafael Herrera[tt,uu], Martin Gilpin[a], Emanuel

15 Gloor[a], Jefferson Hall[vv], David J. Harris[ww], Terese B. Hart[xx,yy], Kuswata Kartawinata[zz,aaa], Lip Khoon

16 Kho[bbb], Kanehiro Kitayama[ccc], Susan G. W. Laurance[ddd], William F. Laurance[ddd], Miguel E. Leal[eee],

17 Thomas Lovejoy[ggg], Jon C.Lovett[a], Faustin Mpanya Lukasu[hhh], Jean-Remy Makana[qq], Yadvinder

18 Malhi [iii], Leandro Maracahipes[jjj], Beatriz S. Marimon[kkk], Ben Hur Marimon Junior[kkk], Andrew R.

19 Marshall[lll,mmm], Paulo S. Morandi[kkk], John Tshibamba Mukendi[hhh], Jaques Mukinzi[qq,nnn], Reuben

20 Nilus[ooo], Percy Núñez Vargas[g], Nadir C. Pallqui Camacho[g], Guido Pardo[qqq], Marielos Peña-Claros[rrr],

21 Pascal Pétronelli[sss], Georgia C. Pickavance[a], Axel D. Poulsen [ttt], John R. Poulsen[hh], Richard B.

22 Primack[uuu], Hari Priyadi[vvv,www], Carlos A. Quesada[r], Jan Reitsma[xxx], Maxime Réjou-Méchain[d],

23 Zorayda Restrepo Correa[kk], Ervan Rutishauser[yyy], Kamariah Abu Salim[zzz], Rafael P. Salomão[aaaa],

24 Ismayadi Samsoedin[bbbb], Douglas Sheil[h,cccc], Rodrigo Sierra[dddd], Marcos Silveira[eeee], J. W. Ferry Slik[zzz],

25 Lisa Steel[ffff], Hermann Taedoumg[c], Sylvester Tan[gggg], John W. Terborgh[hh], Sean C. Thomas[hhhh],

26 Marisol Toledo[rrr], Peter Umunay[iiii], Luis Valenzuela Gamarra[f], Ima Célia Guimarães Vieira[aaaa],

27 Vincent A. Vos[qqq,], Ophelia Wang[kkkk], Simon Willcock[llll], Lise Zemagho[c]

28

29   Author affiliations:

30   [a]School of Geography, University of Leeds, Leeds, UK, [b]Department of Geography, University

31   College London, London, UK,[c]Plant Systematic and Ecology Laboratory, University of Yaounde I,

32   Cameroon, [d]Université Paul Sabatier CNRS, Toulouse, France, [e]United Nations Environment

33   Programme World Conservation Monitoring Centre, Cambridge, UK, [f]Jardín Botánico de Missouri,

34   Oxapampa, Perú,[g]Universidad Nacional de San Antonio Abad del Cusco, Cusco, Perú, [h]CIFOR,

35   Bogor, Indonesia, [i]College of Marine and Environmental Sciences, James Cook University, Australia,

36   [j]Naturalis Biodiversity Center, Leiden, Netherlands,[k]Ecology and Biodiversity Group, Utrecht

37   University, Utrecht, Netherlands, [l]Agence Nationale des Parcs Nationaux, Libreville, Gabon,[m]Institut

38   de Recherche en Ecologie Tropicale, Libreville, Gabon,[n]School of Natural Sciences, University of

39   Stirling, Stirling, UK, [o]Mensuration Unit, Forestry Commission of Ghana, Kumasi, Ghana, [p]Graduate

40   School of Science and Engineering, Kagoshima University, Japan, [q]Instituto de Biodiversidade e

41   Floresta, Universidade Federal do Oeste do Pará, Santarém, Brazil, [r]Instituto Nacional de Pesquisas da

42   Amazônia, Manaus, Brazil, [s]Geography, College of Life and Environmental Sciences, University of

43   Exeter, Exeter, UK, [t]Department of Organismic and Evolutionary Biology, Harvard University,

44   Cambridge, MA, USA, [u]Programa de Ciencias del Agro y el Mar, Herbario Universitario, Venezuela,

45   [v]CIFOR, Guinea, [w]Centre for Ecology and Hydrology, Penicuik, UK, [x]INRA, UMR 'Ecologie des

46   Forêts de Guyane', France, [y]UMR AMAP, IRD, Montpellier, France, [z]UPR BSEF, CIRAD,

47   Montpellier, France, [aa]The University of Edinburgh, School of GeoSciences, Edinburgh, UK,

48   [bb]Biodiversity and Landscape Unit, Gembloux Agro-Bio Tech, Université de Liège, Gembloux,

49   Belgium, [cc]INRA, UMR EEF, Champenoux, France, [dd]Forest Ecology and Forest Management group,

50   Wageningen University, Wageningen, The Netherlands, [ee]Instituto Nacional de Pesquisas da

51   Amazônia, Projeto Dinâmica Biológica de Fragmentos Florestais, Manaus, Brazil, [ff]Herbario Alfredo

52   Paredes, Universidad Central del Ecuador, Quito, Ecuador, [gg]Rougier-Gabon, Libreville, Gabon,

53   [hh]Nicholas School of the Environment, Duke University, Durham, NC, USA, [ii]Inventory &

54   Monitoring Program, National Park Service, Fredericksburgh, VA, USA, [jj]Instituto de Investigaciones

55   de la Amazonia Perúana, Iquitos, Perú, [kk]Servicios Ecosistémicos y Cambio Climático, Jardín

56 Botánico de Medellín, Medellín, Colombia, [ll]Smithsonian Tropical Research Institute, Washington,

57 DC, USA, [mm]Landscape Ecology and Vegetal Production Systems Unit, Universite Libre de

58 Bruxelles, Brussels, Belgium, [nn]Department of Botany & Plant Physiology, Faculty of Science,

59 University of Buea, Buea, Cameroon, [oo]Forest Ressources Management, Gembloux Agro-Bio Tech,

60 University of Liege, Belgium, [pp]Smithsonian Institution, Washington, DC, USA, [qq]Wildlife

61 Conservation Society-DR Congo, Kinshasa I, Democratic Republic of Congo, [rr]Centre de Formation

62 et de Recherche en Conservation Forestiere (CEFRECOF), Democratic Republic of Congo, [ss]Institute

63 of Biology, UNICAMP, Campinas, Brazil , [tt]Centro de Ecologia, Instituto Venezolano de

64 Investigaciones Cientificas, Caracas, Venezuela, [uu]Institut für Geographie und Regionalforschung,

65 Geoökologie, University of Vienna, Austria, [vv]Smithsonian Tropical Research Institute, Panamá,

66 Republic of Panama, [ww]Royal Botanic Garden Edinburgh, Edinburgh, UK, [xx]Lukuru Wildlife Research

67 Foundation, Kinshasa, Gombe, Democratic Republic of Congo, [yy]Division of Vertebrate Zoology,

68 Yale Peabody Museum of Natural History, New Haven, CT, USA, [zz]Herbarium Bogoriense,

69 Indonesian Institute of Sciences, Indonesia, [aaa]Integrative Research Center, The Field Museum,

70 Chicago, IL, [bbb]Tropical Peat Research Institute, Biological Research Division, Malaysian Palm Oil

71 Board, Selangor, Malaysia, [ccc]Kyoto University, Kyoto, Japan, [ddd]Centre for Tropical Environmental

72 and Sustainability Sciences and College of Marine and Environmental Sciences, James Cook

73 University, Cairns, Australia, [eee]Wildlife Conservation Society, Kampala, Uganda, [fff]Center for

74 Tropical Conservation, Duke University, Durham, NC, USA, [ggg]Department of Environmental Science

75 and Policy, George Mason University, Fairfax, VA, USA, [hhh]Faculté des Sciences Agronomiques,

76 Université de Kisangani, Democratic Republic of Congo, [iii]School of Geography and the

77 Environment, University of Oxford, Oxford, UK, [jjj]Universidade Federal de Goiás, Goiânia, Brazil,

78 [kkk]Universidade do Estado de Mato Grosso, Nova Xavantina, Brazil, [lll]Flamingo Land Ltd, Kirby

79 Misperton, UK, [mmm]CIRCLE, Environment Department, University of York, York, UK, [nnn]Salonga

80 National Park, Kinshasa I, DR Congo, [ooo]Sabah Forestry Department, Sabah, Malaysia, [ppp]Jardín

81 Botánico Joaquín Antonio Uribe, Medellín, Colombia, [qqq]Universidad Autónoma del Beni, Riberalta,

82 Bolivia, [rrr]Instituto Boliviano de Investigación Forestal, Santa Cruz de la Sierra, Bolivia, [sss]CIRAD,

83 UMR Ecologie des Forêts de Guyane, France, [ttt]Natural History Museum, University of Oslo, Oslo,

3

84   Norway, [uuu]Department of Biology, Boston University, Boston, MA, [vvv]CIFOR, Bogor, Indonesia,

85   [www]Southern Swedish Forest Research Center, Swedish University of Agricultural Sciences, Alnarp,

86   Sweden, [xxx]Bureau Waardenburg, The Netherlands, [yyy]Carboforexpert, Geneva, Switzerland, [zzz]Faculty

87   of Science, Universiti Brunei Darusallam, Gadong, Brunei, [aaaa]Museu Paraense Emilio Goeldi, Belém,

88   Brazil, [bbbb]FORDA, The Ministry of Forestry and Environment, Bogor, Indonesia, [cccc]Norwegian

89   University of Life Sciences, Aas, Norway [dddd]GeoIS, Quito, Ecuador, [eeee]Museu Universitário,

90   Universidade Federal do Acre, Brazil, [ffff]World Wildlife Fund, Washington, DC, USA, [gggg]CTFS-AA

91   Asia Program, Harvard University, Cambridge, MA, USA, [hhhh]Faculty of Forestry, University of

92   Toronto, Toronto, Canada, [iiii]Yale School of Forestry & Environmental Studies, New Haven, CT,

93   USA, [jjjj]Andes to Amazon Biodiversity Program, Puerto Maldonado, Perú, [kkkk]School of Earth

94   Sciences and Environmental Sustainability, Northern Arizona University, Flagstaff AZ, USA,

95   [llll]Department of Life Sciences, University of Southampton, Southampton, UK

96

97

98

99

100

101

102

103

104

105

106

107

108

109

110

111

112

Supporting materials for Sullivan et al.

Contents

146

147

148

149 **Supplementary methods**

150 Plot selection

151 Plots were obtained from a global dataset of forest inventory plots [1] surveyed using standardised field

152 methods [2]. Plots were 1 ha (except for four that were 0.96ha), and were all located in old-growth,

153 closed-canopy, *terra firme* forests, with mean annual temperature of ≥20°C and mean annual

154 precipitation of ≥1300mm. Thus, montane, swamp, peatland and seasonally flooded forest were

155 excluded. Plots known to have been subject to anthropogenic disturbance were also excluded. This

156 enabled us to focus on carbon-diversity relationships within lowland *terra firme* tropical forest,

157 avoiding major climatic, anthropogenic and hydrological factors that could confound these

158 relationships. Having accurate measures of diversity was important for the purposes of this study, so

159 plots were only included if >80% of trees were identified to genus level and >60% of trees were

160 identified to species level. Identification rates were similar amongst continents (median identification

161 rates to species level: South America = 92.5%, Africa = 93.5%, Asia = 93.1%). We excluded

162 transects >500m in length or <20m in width, and any plot known to contain more than one soil type,

163 and only included non-contiguous samples if within 500m of each other. In each plot all stems

164 ≥100mm diameter were measured, and identified to species level where possible. Where a plot had

165 been surveyed multiple times we normally used the initial census, as these were typically

166 accompanied by botanists so were expected to have the highest proportion of identified stems, except

167 where there was a specific reason (e.g. failure of first census to meet selection criteria) to use a later

168 census.

169 Environmental variables

170 We used soil data from 0-30 cm depth, and used total exchangeable bases (TEB; measuring soil

171 fertility), carbon: nitrogen ratio (C:N ratio; a useful proxy of available phosphorus) and soil texture as

172 explanatory variables in analysis. Plots were assigned a reference soil group according to the World

173 Reference Base soil classification system [3], using data from published sources e.g. [4,5] where available.

174 When these data were not available, the reference soil group as mapped in the Harmonised World Soil

175   Database [6], or SOTER [7] for the Democratic Republic of the Congo, was used. Results are similar when

176   only dominant soil groups are used (Supplementary Fig. 20). Then, the particle size and TEB data for

177   the nearest soil unit of the same reference soil group were extracted from the HWSD or SOTER. C:N

178   data were extracted from the Digital Soil Map of the World, or SOTERLAC or SOTER where available.

179   We extracted mean annual precipitation (MAP) and mean annual temperature (MAT) from the

180   WorldClim database [8] at 30' ($\approx$ 1km) resolution. Temperature data were corrected using the lapse rate

181   Δ temperature = 0.005°C m^{-1} to account for differences between plot elevation and the mean elevation

182   of WorldClim grid-cells. We also calculated cumulative water deficit (CWD), a measure of water

183   stress experienced in the dry season. This was done using mean monthly precipitation from

184   WorldClim and mean monthly potential evapotranspiration (PET, 1980-2010 average) from CRU

185   TS3.22 [9]. The water balance for each month (t) was calculated as $CWD_t = min(0, CWD_{t-1} +$

186    $Precipitation_t - PET_t)$. This model was run recursively over a period of 12 months, starting in the

187   wettest month of the year, with the starting water balance assumed to be zero. The minimum CWD_t

188   value across the year represents the greatest drought stress experienced by plants, and is referred to as

189   CWD.

190

191   <u>Estimating diversity</u>

192   Although we applied stringent selection criteria to ensure that the diversity measures included in this

193   study were largely based on fully identified taxa, it was seldom possible to fully identify all taxa in a

194   plot, as local species pools frequently exceed 1000 tree taxa in the tropical forest domain [10]. Some

195   unidentified stems could safely be considered to be additional taxa and added to richness estimates as

196   botanists had assigned them to morphospecies, or had identified them to a higher taxonomic level not

197   otherwise represented in the plot. We assigned remaining unidentified stems to discrete taxa based on

198   the ratio of taxa per stem based on stems that were fully identified to a given taxonomic level. This

199   procedure was necessary to ensure that richness estimates did not simply reflect the proportion of

7

200   stems that could be fully identified. The formulas for deriving richness estimates at different

201   taxonomic levels are thus:

202   Species richness = $I_s + M_s + a + b + [U_s . P_s]$,

203   Genus richness = $I_g + a + [U_g . P_g]$,

204   Family richness = $I_f + [U_f . P_f]$,

205   Where I = richness of stems identified to a given taxonomic level, M_s = morphospecies richness, a =

206   richness of stems unidentified to genus level but unique representatives of a particular family, b =

207   richness of stems unidentified to species level but unique representatives of a particular genus, U

208   =number of stems remaining unidentified at a given taxonomic level, P = number of taxa (at given

209   taxonomic level) per identified stem, and s, g and f subscripts denoting species, genus and family

210   respectively. [] denotes rounding to the nearest integer.

211   These formulas give richness per unit area. Richness per n stems was estimated using individual based

212   rarefaction at both plot (1 ha) and subplot (0.04 ha) scales. At plot scale, richness was expressed per

213   300 stems, while at subplot scale richness was expressed per 10 stems.

214   We calculated diversity metrics representing the three most commonly used Hill numbers [11], richness

215   (^{0}D), Shannon diversity (^{1}D = exp(H'), where $H' = -\sum p_i \, log \, p_i$, with p_i the proportion of stems

216   belonging to species i) and Simpson diversity (^{2}D = $1/\lambda$, where $\lambda = \sum p_i^2$), as these give different

217   weightings to rare versus dominant taxa, with higher Hill numbers giving greater proportional weight

218   to dominant taxa. In addition, we calculated Fisher's α, as it is commonly used to explore diversity in

219   tropical forests. Fisher's α is a constant derived from the log series $S = \alpha \ln (1+N/\alpha)$, where S is the

220   number of species in the sampled community and N is the number of individuals sampled. Analyses

221   with taxon richness (^{0}D) and Fisher's α have been presented in the main text, with analysis of ^{1}D and

222   ^{2}D presented in supporting materials.

223

224   Analysing beta diversity

225   We used Sørensen index to quantify beta diversity between pairs of plots. These pairwise similarities

226   were related to the geographic distance between pairs of plots using a generalised linear model with a

227   binomial errors and a log-link function following [12]. Fitting exponential distance decay models as

228   generalised linear models in this way avoids the problem of log-transforming zero similarity values,

229   with a binomial error structure appropriate as similarity values are bounded to vary between zero and

230   one [12]. Models were constructed for each continent. The significance of parameter estimates was

231   assessed by resampling the data 10000 times with replacement. Following [12] we excluded identical

232   sites pairs with zero geographic distance and identical tree communities from bootstrap samples as

233   these lie outside the original sampling frame.

234   We also investigated how Fisher's alpha in each continent increased with the number of samples or

235   the distance around a plot, repeating the methods of [13] on our dataset to investigate whether the

236   patterns of diversity accumulation over space they observe are also evident in our data.

237   Incomplete species identifications pose a challenge to the calculation of beta diversity as it means that

238   not all the species pool have been sampled. A wide range of beta diversity metrics, including

239   Sørensen index, show an approximately linear relationship between undersampling of taxa and bias in

240   the beta diversity metric [14]. Because of this we excluded sites with <90% of stems identified to species

241   level from our analysis of beta diversity; this threshold was a compromise between maintaining a

242   large sample of plots and reducing bias caused by undersampling of taxa. This threshold gave a

243   sample size of 99 plots in South America, 105 plots in Africa and 23 plots in Asia. Synonymous

244   species names pose a further challenge, as treating two synonyms as separate species would inflate

245   beta diversity, and no universal adjudicated list exists for all tropical plants. We used the R package

246   Taxonstand [15] to compare species names with those in The Plant List (www.theplantlist.org) and

247   remove identified synonyms. However, 28.5% of identified stems remained unresolved (i.e. the

248   species name was present in The Plant List but it was uncertain whether the species name was a

249   synonym) in Asia after using Taxonstand, compared to 0.3% in South America and 0.6% in Africa,

9

250   indicating that further botanical work is required in Asia to resolve these synonyms. We compared

251   unresolved species in Asia against The Asian Plant Synonym Lookup

252   (phylodiversity.net/fslik/synonym_lookup.htm) in a further attempt to remove synonyms. Following

253   this, 5.2% of identified stems in Asia remained unresolved.

254   <u>Statistical analysis</u>

255   We conducted analyses at three spatial scales, firstly comparing carbon and diversity among

256   continents, secondly, assessing relationships between carbon and diversity between 1ha plots within

257   each continent, and finally assessing carbon – diversity relationships between 0.04 ha subplots within

258   1 ha plots.

259   Differences in carbon-storage and diversity metrics between continents were assessed by modelling

260   each response variable of interest as a function of continent in a linear modelling framework, where

261   continent was a factor with three levels. Area based taxon richness are count data, so were modelled

262   using generalised linear models with negative binomial errors (due to overdispersion) and a log link

263   function. ^{1}D (species level), ^{2}D (species level) and Fisher's α were square root transformed prior to

264   modelling to homogenise variances and ensure normality of residuals. We tested for significant

265   differences between continents using Tukey's all-pair comparisons, implemented in the R packages

266   multcomp [16].

267   We then conducted Kendall's tau correlations between carbon and each diversity metric to assess

268   univariate relationships, using plot level data from each continent in turn. Kendall's tau was chosen as

269   it is non-parametric, so does not assume bivariate normality, and can handle ties. This analysis

270   involved computing 13 tests for each continent, so there is therefore some risk of significant

271   relationships appearing by chance. We used false discovery rate control to adjust P values for multiple

272   testing, and present both corrected and uncorrected P values. We performed power analysis using the

273   R package pwr [17] to assess the smallest effect size (Pearson's r) that could be detected with 80%

274   power given the sample size in each continent. Values of r were converted to τ using the lookup table

275   in [18].

276   The univariate correlations examined whether diversity metrics were spatially congruent with carbon.

277   However, other environmental variables acting on carbon or diversity metrics could enhance or

278   obscure any underlying mechanistic relationship. We therefore conducted a multivariate analysis

279   where carbon was modelled as a function of diversity metrics, climate and edaphic variables. This

280   analysis was performed separately for each continent. Diversity metrics were highly correlated with

281   each other (mean Pearson's $r = 0.833$), so one model was constructed per diversity metric. We

282   included cumulative water deficit (CWD), mean annual temperature (MAT), mean annual

283   precipitation (MAP) as climate variables; we did not include other variables relating to precipitation

284   seasonality as they were strongly correlated with CWD. No plots in Asia experienced CWD different

285   from zero, so CWD was not included in models for there. We used Principal Component Analysis to

286   collapse variation in soil texture into two orthogonal axes, which collectively explained 95.4% of

287   variation in soil texture. Axis one (PCA1) was positively correlated with the amount of sand, while

288   axis two (PCA 2) was correlated with the amount of silt and negatively correlated with the amount of

289   clay (Supplementary Table 1). We also included the sum of total exchangeable bases (TEB) and the

290   carbon: nitrogen ratio (C:N). Explanatory variables were centred and scaled to have a mean of zero

291   and a standard deviation of one. The basic equation for these models was thus

292    $\log(\text{carbon}) = a + \beta_1\text{Diversity metric} + \beta_2\text{CWD} + \beta_3\text{MAP} + \beta_4\text{MAT} + \beta_5\text{PCA1} + \beta_6\text{PCA2} + \beta_7\text{TEB} +$

293    $\beta_8\text{C:N} + \varepsilon$

294   We used MuMIn [19] to fit all valid simplifications of this global model. Each model was ranked based

295   on AIC_C, from which the Akaike weight of each model i was calculated (ω_i). The parameters of the

296   best supported models (defined as the models required for cumulative sum of $w_i = 0.95$, known as the

297   95% confidence set) were averaged, while the support for individual explanatory variables was

298   assessed by summing to ω_i of models in which that variable appeared.

299   Spatial autocorrelation in residuals of these OLS models was examined by plotting correlograms

300   using the R package ncf [20]. Positive short range and negative long-range residual autocorrelation was

301   evident in South America, suggesting the presence of strong environmental gradients. Residual spatial

302 autocorrelation was less strong in Africa, and weakest in Asia, but was present in all continents. We

303 repeated the above modelling procedures using simultaneous autoregressive error models (SAR),

304 implemented in spdep [21]. These were selected because of good performance in evaluations by [22], with

305 error models selected, as opposed to lag or mixed SARs, as [23] found they performed better regardless

306 of the mechanism generating spatial autocorrelation. We selected the best neighbourhood distance for

307 each global model by fitting models with maximum neighbourhoods distances varying in 20km

308 increments from 20km to 1000km, and selecting the neighbourhood distance that gave the lowest

309 AIC_C. Although all SAR models had lower AIC values than OLS models, we present results from

310 both OLS and SAR models, as it has been argued that spatial models are not necessarily more correct

311 than non-spatial models [24].

312 We assessed fine-scale relationships between diversity and carbon by using multiple regression to

313 model ln (carbon) in 0.04ha subplots as a function of diversity and the number of stems in the subplot,

314 with a second order polynomial used for the number of stems to capture potentially saturating

315 relationships. Explanatory variables were natural log transformed to allow comparison with results of

316 [25]. We ran these models in each 1ha plot where subplot level was available (n = 266). We tested

317 whether the mean coefficient was different from zero using one-sample Wilcoxon tests, and

318 calculated 95% confidence intervals from 10000 bootstrap resamples with replacement. Running

319 separate models for each plot allowed us to capture variability in fine scale relationships between

320 plots. However, the overall mean relationship between diversity and carbon at subplot scale could be

321 more robustly assessed using mixed effects models with random coefficients. This assumes that

322 coefficients in plot j come from a normal distribution, $\beta_j \sim Normal(\mu_\beta\ \sigma^2_\beta)$, where μ_β is the mean value

323 of the coefficient across plots, and σ^2_β is the variance of the coefficient across plots. We relax the

324 assumption of independence between coefficients, so that pairs of coefficients in the same plot are

325 assumed to come from a multivariate normal distribution with correlations between coefficients

326 estimated in a variance-covariance matrix. Mixed effects models were implemented using the R

327 package lme4 [26].

328

329   **Supplementary Discussion – Examining support for mechanisms underpinning diversity-carbon**

330   **relationships**

331   Our results show a weak positive relationship between diversity and carbon storage at small spatial

332   scales (among 0.04 ha subplots within 1 ha plots), but no pan-tropically consistent relationship among

333   1 ha plots, even after controlling for potentially confounding environmental variation and spatial

334   autocorrelation. These results pose two questions. Firstly, which mechanisms underlie the positive

335   diversity-carbon relationship between 0.04 ha subplots? And secondly, why do these mechanisms

336   appear to only operate at small spatial scales? These questions are best investigated with long-term

337   experiments in tropical forests, however, we can evaluate whether correlative results from our

338   observational dataset are consistent with the operation of niche complementarity and selection effects

339   at 0.04 ha and 1 ha scales.

340   <u>Evidence for niche complementarity</u>

341   Positive relationships between biodiversity and ecosystem function have been hypothesised to arise

342   through two general mechanisms, niche complementarity and the selection effect. The niche

343   complementarity hypothesis proposes that differences in resource use by species allows diverse

344   communities to use available resources more efficiently than less diverse communities [27]. For

345   example, in low diversity temperate forests, complimentary canopy architecture has been found to

346   drive a positive relationship between diversity and productivity [28]. In tropical forests attempts to

347   assess the role of niche complementarity have focused on relating above-ground live carbon storage to

348   the functional diversity of tree communities [29,30], with the expectation that more functionally diverse

349   species assemblages should be able to partition resources more effectively. However, these studies

350   found no relationship between carbon storage and functional diversity [29,30].

351   Quantifying functional diversity in tropical forests is challenging due to the shortage of available trait

352   data. We used two approaches to quantify functional diversity, (i) the standard deviation of wood

353   density (SD_{WD}) in a subplot or plot, and (ii) a multivariate functional diversity metric (FDM) using

354   both the wood density and the maximum diameter of each species in a subplot or plot.

13

355   For the SD_{WD} we used published wood density values [31,32], and commonly used methods to select

356   genera-level wood density in cases when literature values for a given species were unavailable [33-35]. It

357   would be preferable to use local trait data [36] but as these are not available for many plots it is

358   necessary to use literature values for pan-tropical studies [29]. Wood density provides a proven proxy

359   for life history strategy in tropical forests [37], since denser wooded trees tend to be slower growing, less

360   light demanding and potentially larger than species with lower wood density [38,39], and variation in

361   wood density is closely related to variation in leaf traits [40] and demographic traits [41]. We therefore

362   expect that the potential for niche complementarity is greater in species assemblages with more

363   variation in wood density.

364   The relationship between carbon storage and SD_{WD} at the 0.04 ha scale within 1-ha plots was variable

365   but significantly negative overall. At the 1 ha scale the relationship was significantly negative in all

366   three continents (Fig. S1). At both scales, SD_{WD} was negatively related to mean wood density (Fig.

367   S2), indicating that the more variable plots were increasingly composed of species with 'fast' life

368   history strategies. These plots potentially have high rates of stem turnover, and thus shorter biomass

369   residence time [42]. When we included community weighted mean wood density as a covariate to

370   account for this, the negative relationship between carbon storage and wood density standard

371   deviation among 0.04 ha subplots was weaker but still significantly negative ($P < 0.001$). Negative

372   relationships among 1 ha plots also weakened in all continents (non-significantly negative in South

373   America and Africa ($P \geq 0.177$), significantly negative in Asia ($P = 0.004$). SD_{WD} was also negatively

374   related to the community weighted mean of maximum diameter at both scales (Fig. S3), indicating

375   that plots with a greater variety of tree life history strategies were increasingly composed of smaller

376   tree species.

377   We then estimated functional diversity using the FDM, calculated following [43]. For this, we follow

378   Cavanaugh et al. [29] and define functional diversity in terms of the wood density and maximum

379   diameter of each species in an assemblage (they worked at genus level). Thus, following Fauset et al.

380   [44], we estimated maximum diameter as the 95th percentile diameter of species with a least 20 stems in

381   the dataset. We used species-level maximum diameters were available, with genus-level estimates

14

382   used for species that occurred too infrequently to estimate species level maximum diameter, and

383   family-level estimates used when there was no genus-level estimate. We estimated maximum

384   diameter for each genus and family using the same methods as for species-level estimates. We used

385   this trait data to construct a functional dissimilarity matrix, where the dissimilarity of pairs of species

386   based on their traits was quantified using Gower distance. This dissimilarity matrix was converted

387   into a dendrogram using average linkage. FDM was calculated as the sum of branch lengths of a

388   dendrogram containing all species in a plot or subplot divided by the sum of branch lengths of a

389   dendrogram containing all species in the potential source pool, defined as all species in our dataset

390   found in a given continent. Thus, FDM is equal to one when all the trait diversity in the source pool of

391   species is found in in the subset of species in a subplot or plot, and decreases towards zero as

392   increasingly large amounts of trait diversity are missing from the subset of species.

393   Our FDM metric showed an overall weak positive relationship between functional diversity and

394   carbon storage at the 0.04ha scale (Fig. S1), which remained when community-weighted mean wood

395   density was included as a covariate ($\beta = 2.6$, $P < 0.001$). However, at the 1 ha scale, FD and carbon

396   storage were unrelated, even when community-weighted mean (CWM) wood density was included as

397   a covariate ($P \geq 0.118$). This is consistent with results of previous studies at this scale [29,30], which

398   found no relationship between functional diversity and carbon storage. At both scales FDM was

399   weakly negatively related to community-weight mean wood density (Fig. S2), indicating that the most

400   functionally diverse stands were composed of species with fast life-history strategies. FDM was

401   positively related to the community weighted mean of maximum diameter at 0.04 ha scale but not at 1

402   ha scale. This indicates that at small scales trees are on average larger in more functionally diverse

403   stands. The weak positive relationship between FDM and carbon storage at 0.04 ha but not 1 ha scale

404   is consistent with the scale-dependent operation of niche complimentarily.

405
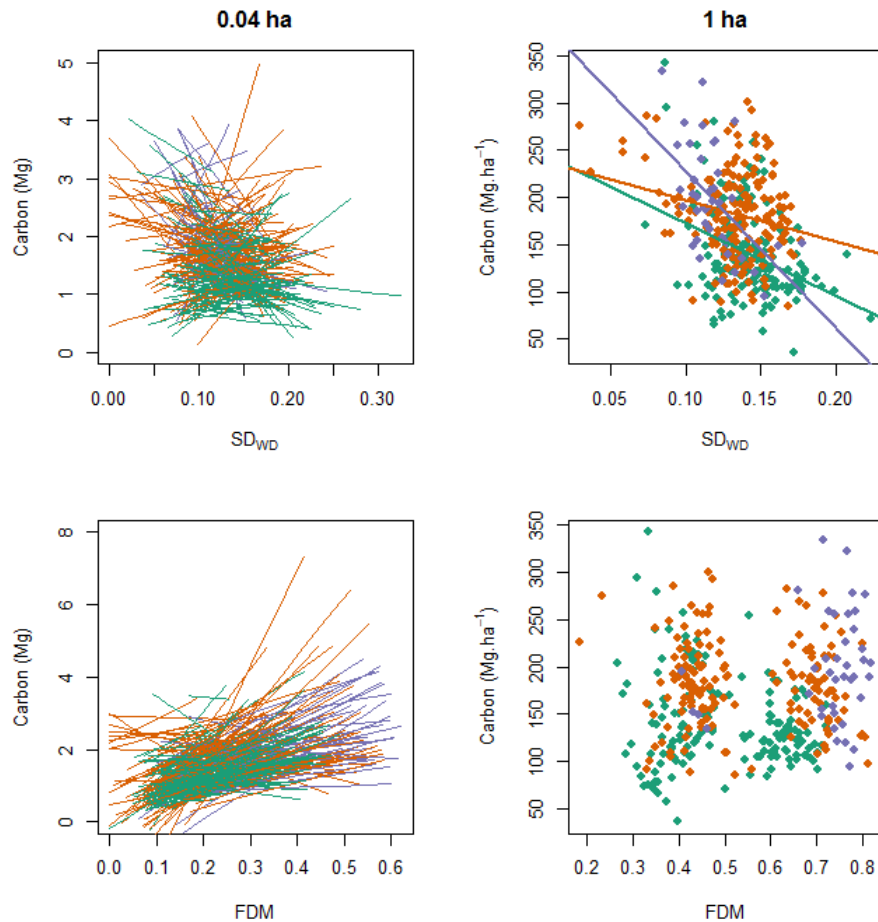
Supplementary Figure 1. Relationship between carbon storage and functional diversity. Functional diversity is quantified either as the standard deviation of wood density among stems within a plot/ sub-plot (SD_{WD}), or using a dendrogram based method where species are clustered according to their wood density and maximum diameter traits (FDM). Relationships are shown for 1 ha plots in each continent (data from South America are shown by green circles, Africa by orange squares, and Asia by purple triangles, regression lines are shown for significant relationships ($P < 0.05$)), and for 0.04 ha subplots in 1 ha plots (regression lines shown for each 1 ha plot, colour scheme same as before). Relationships between wood density SD and carbon are: South America 1 ha, $\beta = -5.0$, $P < 0.001$; Africa 1 ha $\beta = -2.3$, $P = 0.006$; Asia 1ha, $\beta = -9.1$, $P < 0.001$; 0.04 ha mixed effects model, $\beta = -1.1$, $P < 0.001$. Relationships between functional diversity and carbon are: South America 1 ha, $\beta = -0.3$, $P = 0.139$; Africa 1 ha, $\beta = -0.1$, $P = 0.687$, Asia 1 ha, $\beta = 0.5$, $P = 0.236$; 0.04 ha mixed effects model, $\beta = 2.5$, $P < 0.001$.

16
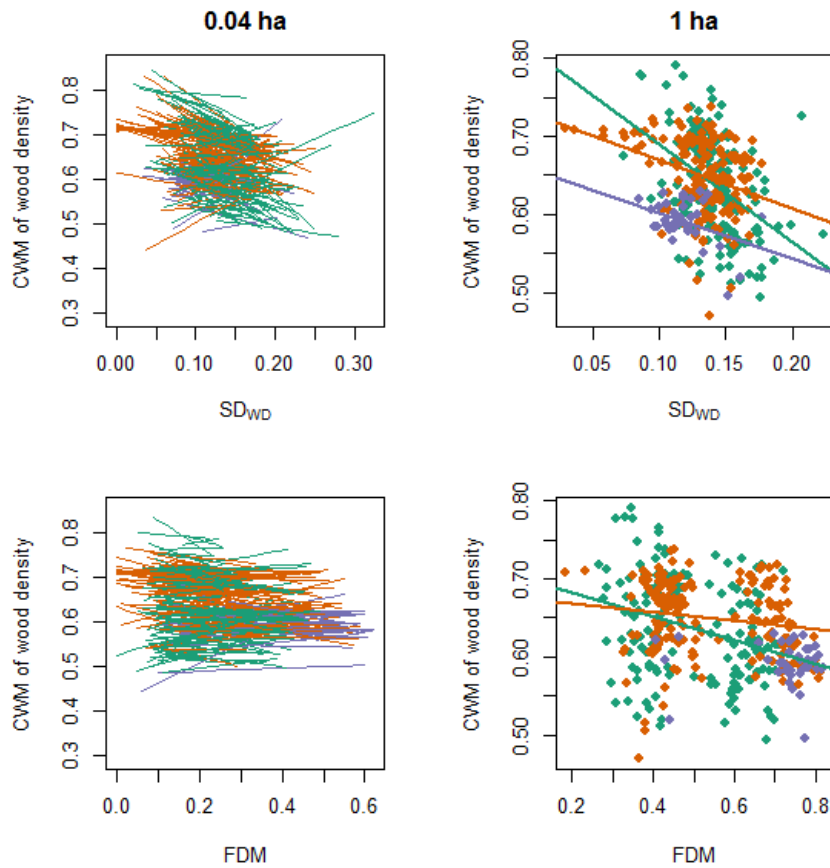
Supplementary Figure 2. Relationship between measures of functional diversity the community weighted mean of wood density. Symbols as in Fig. S1. Relationships between SD_{WD} and CWM of wood density are: South America 1 ha, $\beta = -1.3$, $P < 0.001$; Africa 1 ha, $\beta = -0.6$, $P < 0.001$; Asia 1 ha, $\beta = -0.6$, $P = 0.012$; 0.04 ha mixed effects model, $\beta = -0.31$, $P < 0.001$. Relationships between FDM and CWM of wood density are: South America 1 ha, $\beta = -0.2$, $P < 0.001$; Africa 1 ha, $\beta = -0.1$, $P = 0.0371$; Asia 1 ha, $\beta = <-0.1$, $P = 0.768$; 0.04 ha mixed effects model, $\beta = -0.02$, $P = 0.005$.
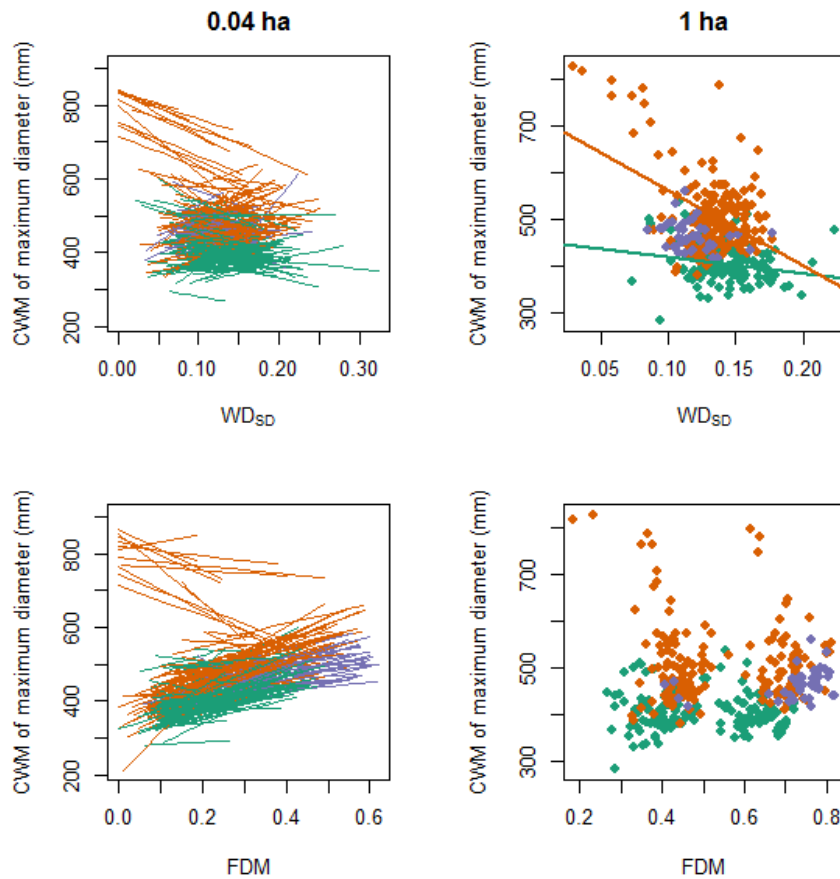
Supplementary Figure 3. Relationship between measures of functional diversity and the functional dominance of species with large maximum diameters. Symbols as in Fig. S1. Relationships between SD_{WD} and community-weighted mean (CWM) of maximum diameter are: South America 1 ha, β = -349, P = 0.0095; Africa 1 ha, β = -1623, P < 0.001; Asia 1 ha, β = -387, P = 0.156; 0.04 ha mixed effects model, β = -34, P < 0.001. Relationships between FDM and CWM of maximum diameter are: South America 1 ha, β = -33, P = 0.181; Africa 1 ha, β = -71, P = 0.137; Asia 1 ha, β = 84.7, P = 0.074; 0.04 ha mixed effect model, β = 263, P < 0.001.

Evidence for the selection effect

A second mechanism by which positive diversity-ecosystem function relationships might be generated

is via the selection effect. The selection effect hypothesis proposes that diverse communities, by

containing a greater proportion of the overall species pool, are more likely to contain dominant

species that contribute strongly to ecosystem function [27]. Species contributions to ecosystem function

are known to be highly uneven in Amazonian forests, where approximately 1% of species are

responsible for 50% of carbon storage [44]. Furthermore, maximum diameter is known to be the most

443   important determinant of species' contribution to carbon storage [44], aside from overall abundance,

444   while pan-tropically plot-level carbon stocks are closely related to the density of large trees (defined

445   as d.b.h. $\geq$ 70 cm) [45]. Thus any positive diversity-carbon relationship could plausibly arise through

446   diverse plots being more likely to contain species with large maximum diameters.

447   Previous attempts to evaluate whether selection effects occur in tropical forests have tested the

448   prediction that carbon storage is related to the functional dominance of species with large maximum

449   diameters or dense wood [29,30]. To begin with, we therefore repeated this approach with our larger pan-

450   tropical dataset (360 plots), using the community weighted mean of wood density and maximum

451   diameter as a measure of functional dominance. We found that at both scales carbon storage increased

452   with the community weighted mean of maximum diameter, as found by previous studies at 1 ha scale

453   [29,30], and also that it increased with the community weighted mean of wood density (Fig. S4), which

454   the previous studies did not detect as a driver of carbon storage [29,30]. However, while this approach is

455   useful and interesting, strictly it is a test of the biomass ratio hypothesis, by which ecosystem function

456   is related to the traits of dominant taxa [46], rather than a test of the selection effect *per se*.
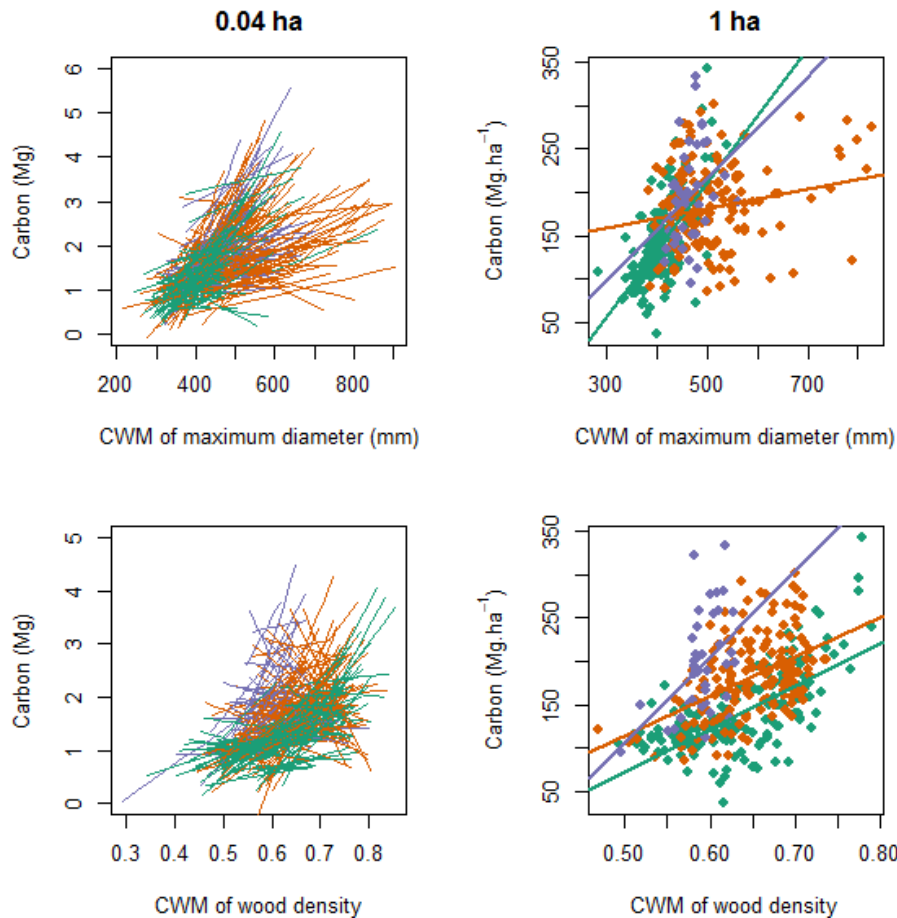
Supplementary Figure 4. Relationship between community weighted mean (CWM) of species traits and carbon storage. The community weighted mean of traits indicates the dominance of species with different trait values within a community. Symbols as in Fig. S1. Relationships between CWM of maximum diameter and carbon are: South America 1 ha, $\beta = 0.0049$, $P < 0.001$; Africa 1 ha, $\beta = 0.0006$, $P = 0.022$; Asia 1 ha, $\beta = 0.0030$, $P = 0.049$; 0.04 ha mixed effects model, $\beta = 0.0029$, $P < 0.001$. Relationships between CWM of wood density and carbon are: South America 1 ha, $\beta = 3.1$, $P < 0.001$; Africa 1 ha, $\beta = 2.8$, $P < 0.001$; Asia 1 ha, $\beta = 5.7$, $P = 0.0005$; 0.04 ha mixed effects model, $\beta = 2.4$, $P < 0.001$.

Another, and directly testable, prediction of the selection effect is that the probability of a community

containing a functionally dominant species increases with species richness. Maximum diameter has

been found to be an important determinant of species' contribution to carbon storage. Of our 1441

species for which the species level maximum diameter could be estimated, 169 (11.7%) had

maximum diameters ≥ 70 cm. The probability of a random sample of s species from this species pool

containing a potentially large tree species (L) is thus $L = 1 - 0.883^{s}$. This means that the probability of

sampling a potentially large tree species rapidly saturates with species richness. For example, at 14

474   species (the median species richness of 0.04 ha subplots) $L = 0.826$, while at 100 species (the median

475   species richness of 1 ha plots) $L > 0.999$. This calculation ignores differences in species composition

476   between continents, so we also estimated the probability of samples of different species richness

477   containing a potentially large species by sampling the tree species in our dataset 3000 times for each

478   species richness increment, with each sample restricted to contain species from a single continent

479   (1000 samples for each continent). We also repeated this procedure with the probability of sampling a

480   species weighted by that species' frequency in a continent. Both approaches gave a similar rapidly

481   saturating curve (Fig. S4), and with a slightly higher probability of sampling large species when

482   species frequency was maintained. Importantly, the probability of a sample containing a potentially

483   large species increases substantially through the inter-quartile range of 0.04 ha species richness

484   values, but for the whole inter-quartile range of 1 ha species richness values samples were almost

485   certain to contain a potentially large species (Fig. S5). Similar inferences obtain when we modelled

486   the probability of subplots containing potentially large tree species was as a function of species

487   richness using binomial generalised mixed models (with plot identity as a random effect): the

488   probability of sampling a large tree species in a 20x20m subplot increased with species richness (Fig.

489   S6), but at the 1 ha scale all but one of our 360 plots contains a potentially large tree species. This

490   further supports the inference that selection effects could plausibly lead to a relationship between

491   diversity and carbon storage at 0.04 ha scale, but that tropical forest 1 ha plots are sufficiently diverse

492   for selection effects to have potentially saturated.

493

494

495

496

497

498

21

499
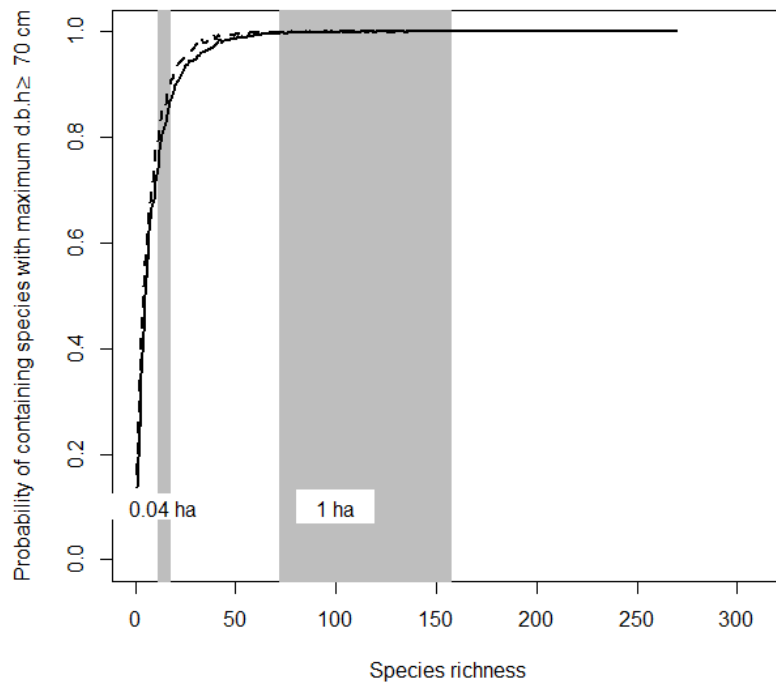
Supplementary Figure 5. Relationship between the species richness of a sample and the probability of that sample containing a potentially large tree species (maximum diameter $\geq$ 70 cm). Probabilities were estimated by randomly sampling the species pool in each continent 1000 times for each continent and species richness increment, with the probability of selecting a species either equal for all species in a continent (solid line) or weighted by the proportion of plots that species was recorded in (dashed line). The interquartile range of species richness in 0.04 ha subplots and 1 ha plots are shown by grey shading.

507

508
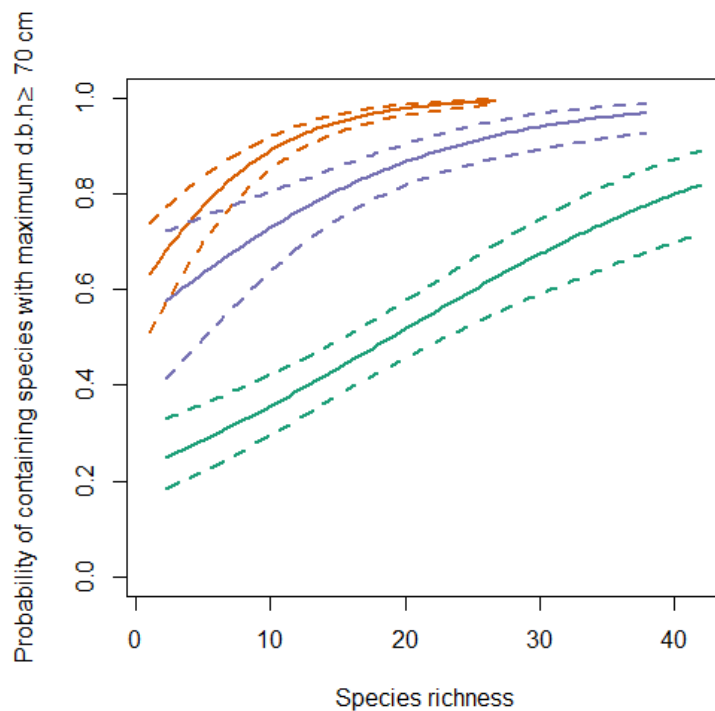
Supplementary Figure 6. Observed relationship between species richness of 0.04 ha subplots and the probability of that subplot containing a potentially large species (maximum diameter $\geq$ 70 cm). Fitted relationships in each continent are from generalised linear mixed effects models with binomial errors (green = South America, orange = Africa, purple = Asia). Standard errors are shown with dashed lines. Model coefficients are: South America, $\beta = 0.066$, $P < 0.001$; Africa, $\beta = 0.173$, $P < 0.001$; Asia, $\beta = 0.088$, $P < 0.001$. Relationships are not shown for 1 ha plots, as all but one of our 360 plots contained a potentially large species.

We find similar results when evaluating the probability of sampling a species with high wood density.

Thus, the probability of sampling a species with wood density ≥ 0.8 g.cm^{-3} increases with species

richness through the range of species richness values found in 0.04 ha subplots, but saturates by the

species richness values found in 1 ha plots (Fig. S7). All but one 1 ha plot contains a species with

wood density ≥ 0.8 g.cm^{-3}, however at 0.04 ha scale there is a positive relationship in all continents

(Fig. S8).

Although the choice of 70 cm as a threshold for maximum diameter is supported by previous work

demonstrating the contribution of trees of this size class to overall biomass [45], the thresholds chosen

for both maximum diameter and wood density are essentially arbitrary. To explore sensitivity to this

choice we also explored the effects using other, substantially different, thresholds. Setting a lower

23

527   threshold naturally means that the probability of sampling a high functioning species saturates at

528   lower species richness, while setting a higher threshold means that it saturates at higher species

529   richness (Fig. S9, Fig. S10). However, for all the thresholds which we investigated, the probability of

530   sampling a high functioning species increased more rapidly with species richness though the range of

531   species richness values found in 0.04 ha subplots than the range of species richness values found in 1

532   ha plots (Fig. S9, Fig. S10).
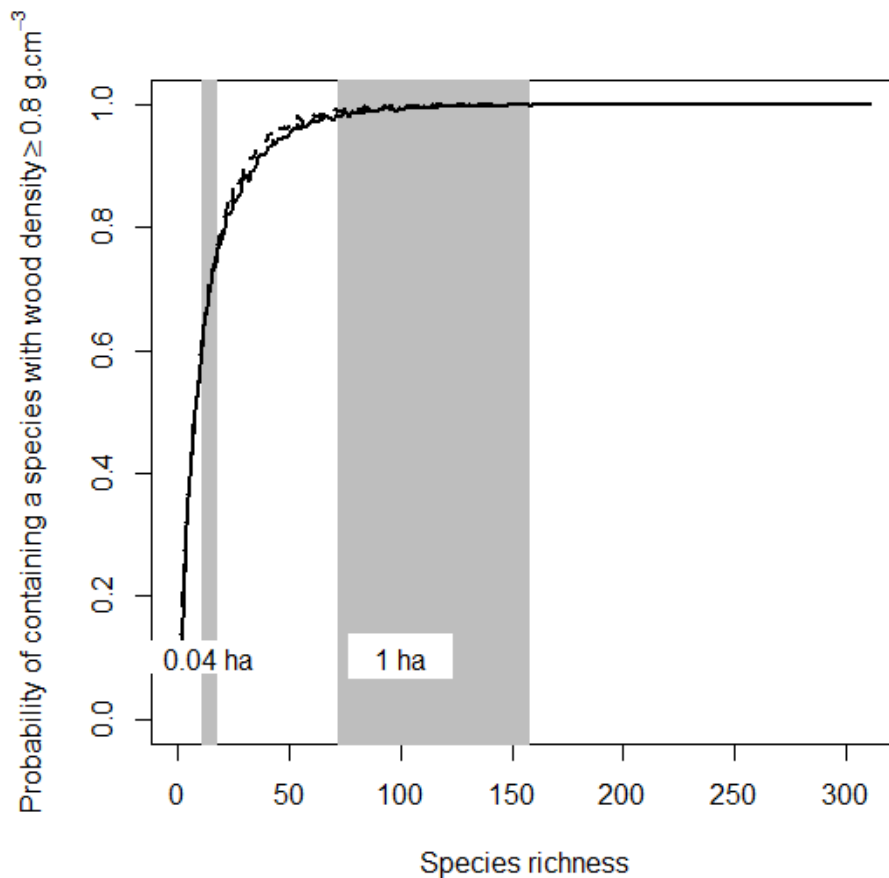
533

534   **Supplementary Figure 7**. Relationship between the species richness of a sample and the probability
535   of that sample containing a species with high wood density (wood density ≥ 0.8 g.cm^{-3}). Probabilities
536   were estimated by randomly sampling the species pool in each continent 1000 times for each
537   continent and species richness increment, with the probability of selecting a species either equal for
538   all species in a continent (solid line) or weighted by the proportion of plots that species was recorded
539   in (dashed line). The interquartile range of species richness in 0.04 ha subplots and 1 ha plots are
540   shown by grey shading.

541

24

542
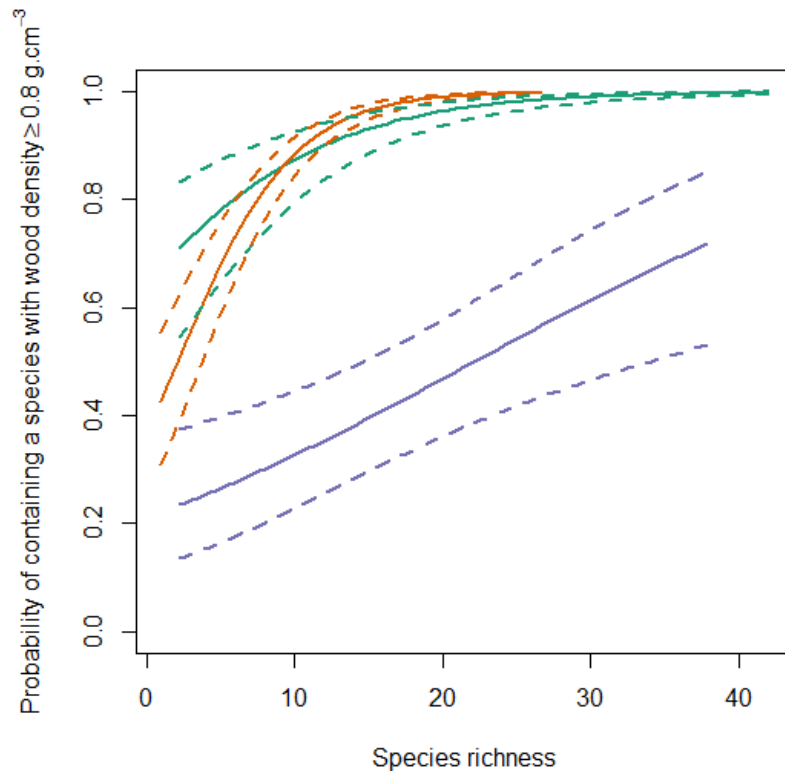
Supplementary Figure S8. Observed relationship between species richness of 0.04 ha subplots and the probability of that sample containing a species with high wood density (wood density ≥ 0.8 g.cm^{-3}). Fitted relationships in each continent are from generalised linear mixed effects models with binomial errors (green = South America, orange = Africa, purple = Asia). Standard errors are shown with dashed lines. Model coefficients are: South America, $\beta = 0.135$, $P < 0.001$; Africa, $\beta = 0.258$, $P < 0.001$; Asia, $\beta = 0.059$, $P = 0.001$. Relationships are not shown for 1 ha plots, as all but one of our 360 plots contained a species with high wood density.

550
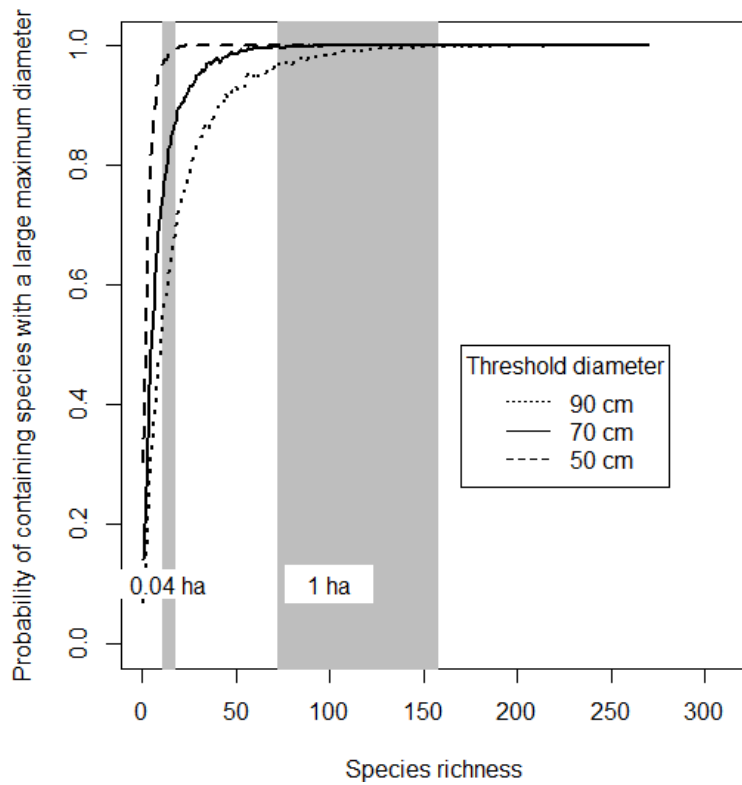
Supplementary Figure 9. Sensitivity of the relationship between the species richness of a sample and the probability of that sample containing a potentially large tree species to the choice of threshold maximum diameter. Probabilities were estimated by randomly sampling the species pool in each continent 1000 times for each continent and species richness increment, with the probability of selecting a species either equal for all species in a continent (solid line). The interquartile range of species richness in 0.04 ha subplots and 1 ha plots are shown by grey shading.
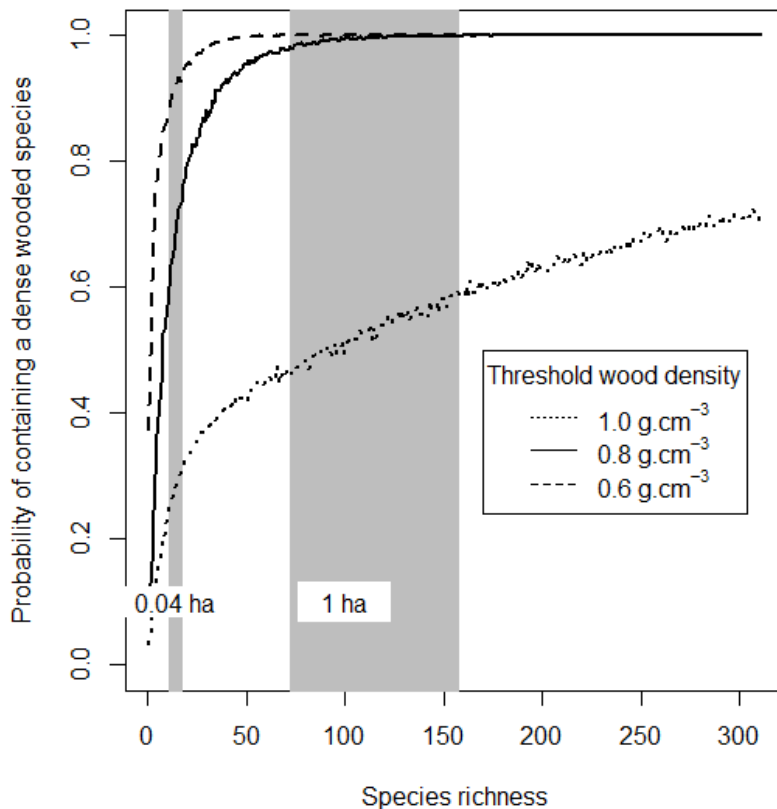
559

560 **Supplementary Figure 10.** Sensitivity of the relationship between the species richness of a sample
561 and the probability of that sample containing a species with high wood density to the choice of
562 threshold wood density. Probabilities were estimated by randomly sampling the species pool in each
563 continent 1000 times for each continent and species richness increment, with the probability of
564 selecting a species either equal for all species in a continent (solid line). The interquartile range of
565 species richness in 0.04 ha subplots and 1 ha plots are shown by grey shading.

566

567

568 Conclusions

569 Our results are consistent with the weak positive relationship between diversity and carbon storage

570 resulting from niche complementarity and/or selection effects, as at this scale we found a weak

571 positive relationship between carbon storage and functional diversity (Fig. S1, consistent with niche

572 complementarity) and between species richness and the probability of sampling a large tree (Fig. S6,

573 consistent with selection effects). We note that positive diversity-carbon relationships at fine scales

574 could also result from density dependent effects, which could arise if pests and pathogens incur a

575 reduced cost on species with low local densities. We found no evidence of either selection effects or

576   niche complementarity operating at the 1-ha scale, which is consistent with both mechanisms being

577   scale dependent. For selection effects this potential scale dependency could arise through the greater

578   number of species as spatial scale increases, as we show that 1 ha plots are already sufficiently diverse

579   for plots to be almost certain to contain a potentially large tree species (Fig. S5).

580   Carbon storage was related to the dominance of wood density and maximum diameter traits in species

581   assemblages (Fig. S3), consistent with the biomass ratio hypothesis where ecosystem function is

582   related to the traits of the dominant taxa. Our results are therefore consistent with previous studies in

583   showing that carbon storage in 1 ha plots is related to functional dominance but not to functional

584   diversity [29,30], and extend these by firstly showing that selection effects potentially saturate so are

585   unlikely to explain functional dominance at 1 ha scales, and secondly by reporting correlations

586   consistent with the operation of both niche complementarity and selection effects at the 0.04 ha scale.

587   Overall, we find support for the operation of niche complementarity and selection effects at 0.04 ha

588   scale but no evidence for their operation at 1 ha scale, although as firm causal inferences cannot be

589   drawn from correlative observational studies such as this substantial uncertainty remains about the

590   role of niche complementarity and selection effects in tropical forests. The potential scale dependency

591   of both mechanisms is consistent with the central finding of our pan-tropical analysis: except at the

592   very smallest scales, across and within the three main tropical forest continents, above-ground live

593   carbon storage and tree diversity are decoupled.

594

595

596

597

598

599

600

601

602

603 **Additional figures and tables**
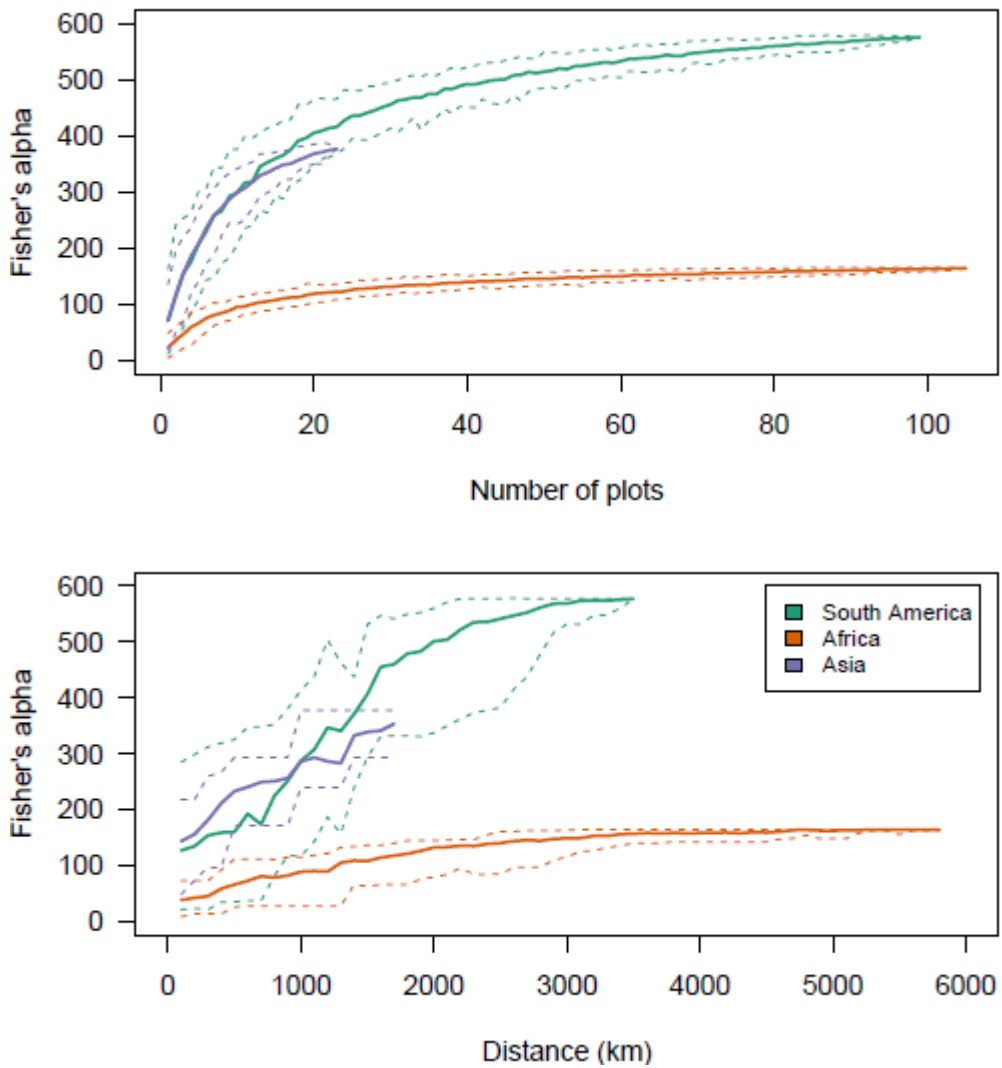
604

605

606 **Supplementary Figure 11.** Increase in diversity (Fisher's α) with increasing sample size of plots and
607 increasing geographic distance around plots. For each sample size a random selection of *n* plots was
608 drawn from the pool of available plots in each continent, while for each distance, a random plot was
609 selected and all plots within a given distance of it were selected. This was repeated 100 times for each
610 sample size and distance. Solid lines show mean values and dashed lines 95% confidence limits from
611 these samples.

612
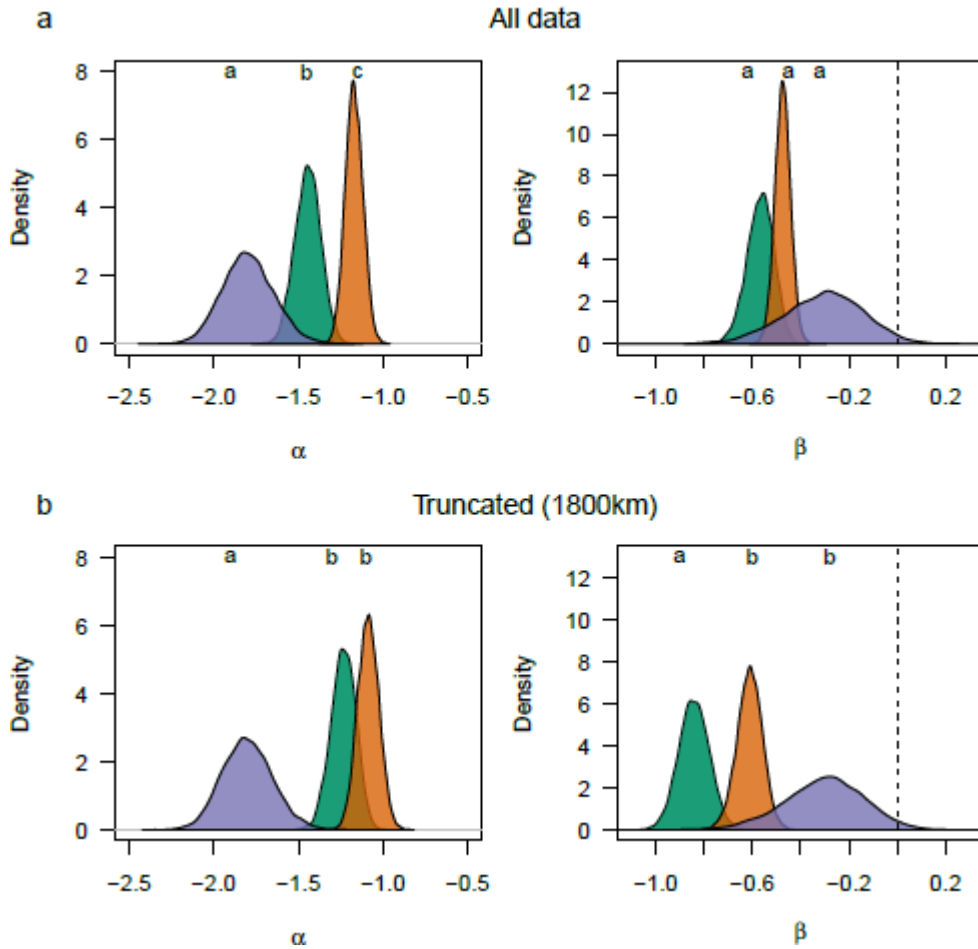
Supplementary Figure 12. Coefficients of generalised linear models of species similarity (Sørensen index) against distance, with α being the model intercept and β being the gradient. The distributions of parameters from 10000 bootstrap samples are shown. Models for South America are in green, Africa orange and Asia purple. Asia has a significantly lower intercept than Africa and South America, and when data were truncated a significantly shallower gradient than South America.

629
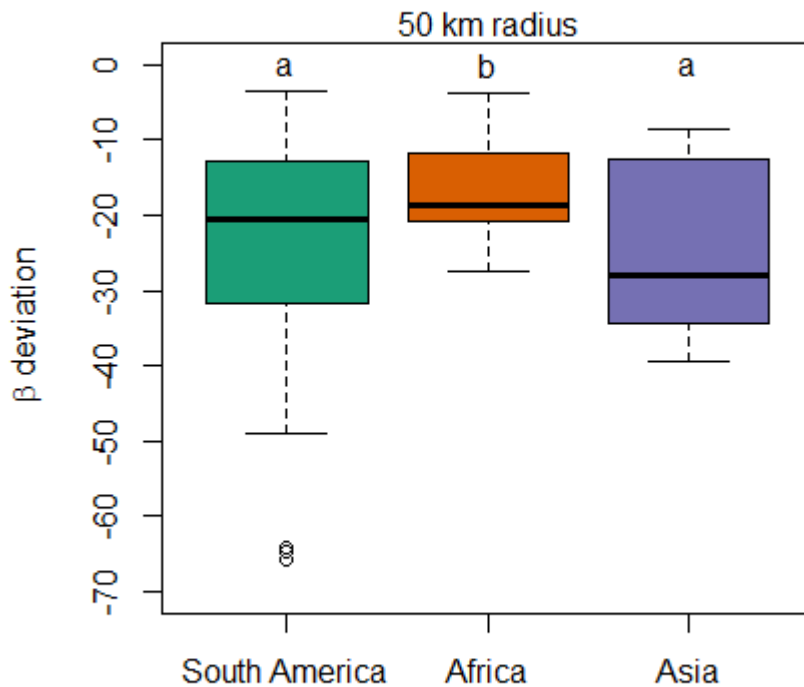
Supplementary Figure 13. Variation in the standardised effect size of the difference between observed and expected Sørensen index values (β deviation). β deviation values below zero indicate that forest stands are less similar than expected after controlling for the effect of gamma diversity. Expected values were generated by using a null model that randomly shuffles individual trees among plots within a sample area, while maintaining the number of stems in each plot and the overall gamma diversity and relative abundance of species in the sample area [47]. β deviation was estimated for each plot, with the sample area defined as a 50 km radius around that plot. The null model was run for 1000 iterations for each plot. Beta deviation differed significantly amongst continents (Kruskal-Wallis, $\chi^2 = 13.7$, $P = 0.001$). Different letters indicate significant differences between continents (pairwise Mann-Whitney tests with false discovery rate correction, $P < 0.05$). Beta deviation in all continents was significantly lower than zero (one sample Wilcoxon tests, $P < 0.001$).

641
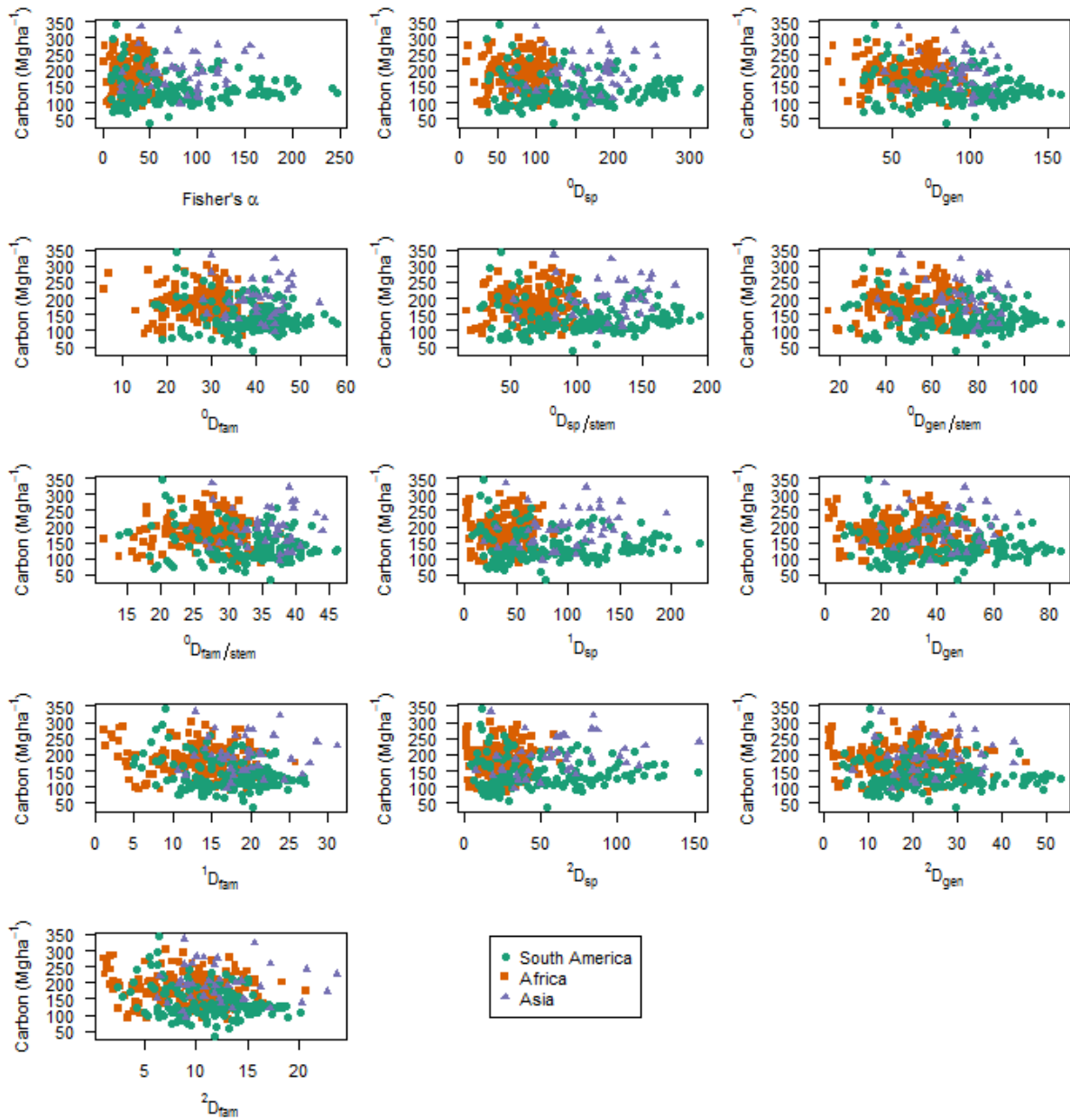
Supplementary Figure 14. Relationship between carbon and each diversity metric in plots in South America (green circles), Africa (orange squares and Asia (purple triangles). Diversity Hill numbers have been calculated for different taxonomic levels (sp= species, gen = genus, fam = family) and by area or per 300 stems (taxa/ stem). There are no significant relationships between any of these diversity metrics and forest biomass carbon.
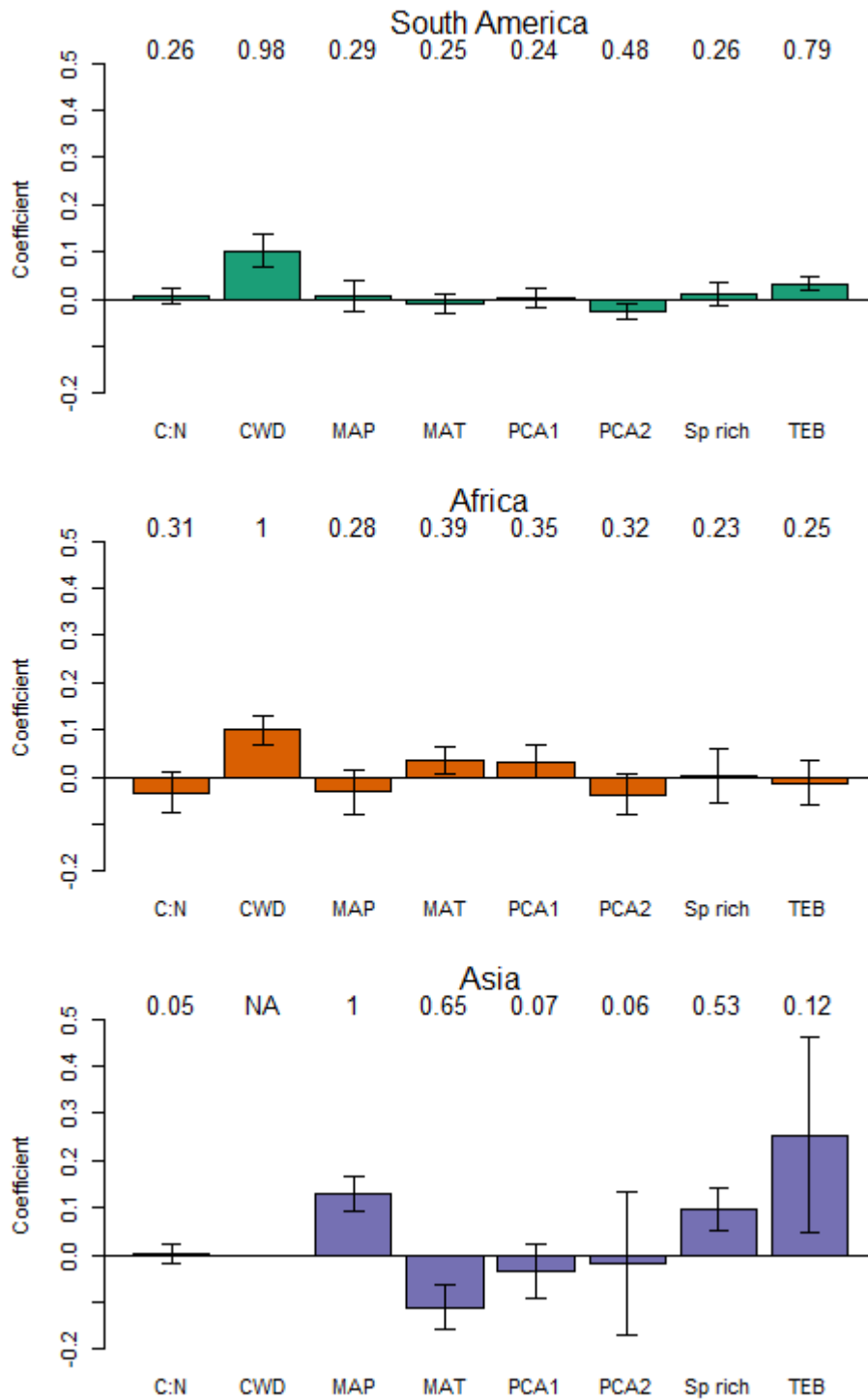
Supplementary Figure 15. Average model coefficients from simultaneous autoregressive error model of carbon storage in 1 ha plots as a function of species richness (Sp rich), climate (CWD, MAP, MAT) and soil (C:N, PCA1, PCA2, TEB). The sum of AIC_C weights of models containing a variable are shown above each variable. Coefficients of ordinary least squares models and models with other diversity metrics are presented in Table S4.

33
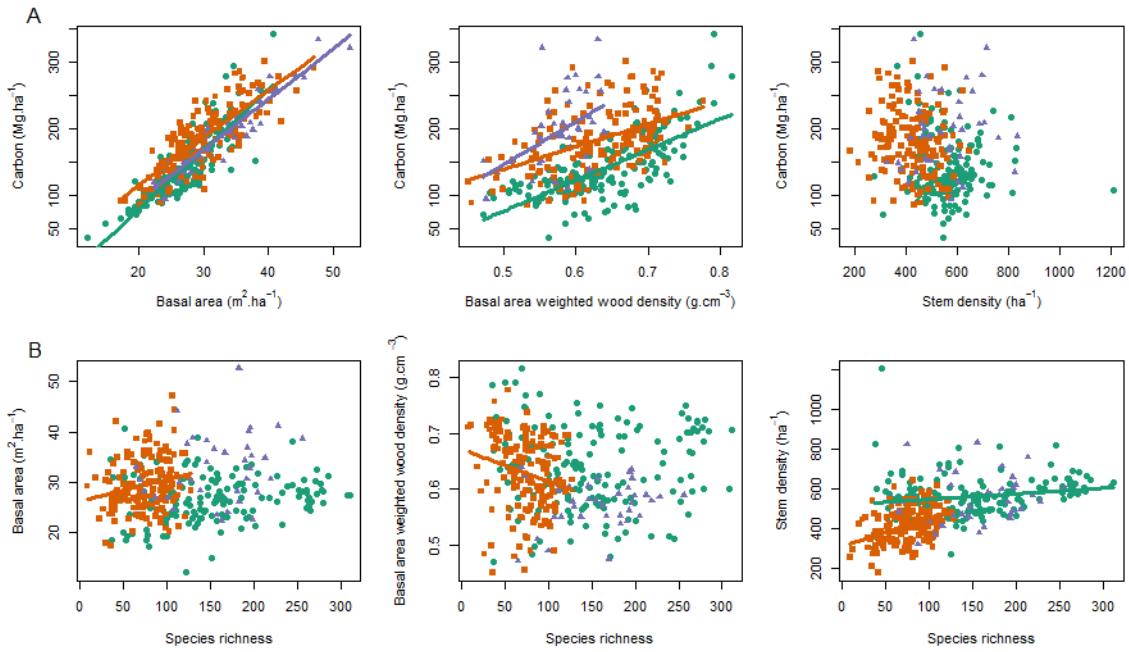
Supplementary Figure 16. (A) Relationship between carbon storage and stand structure and (B) relationship between stand structure and species richness in 1 ha plots. Data from South America are shown by green circles, Africa by orange squares, and Asia by purple triangles. Regression lines show significant relationships.

665
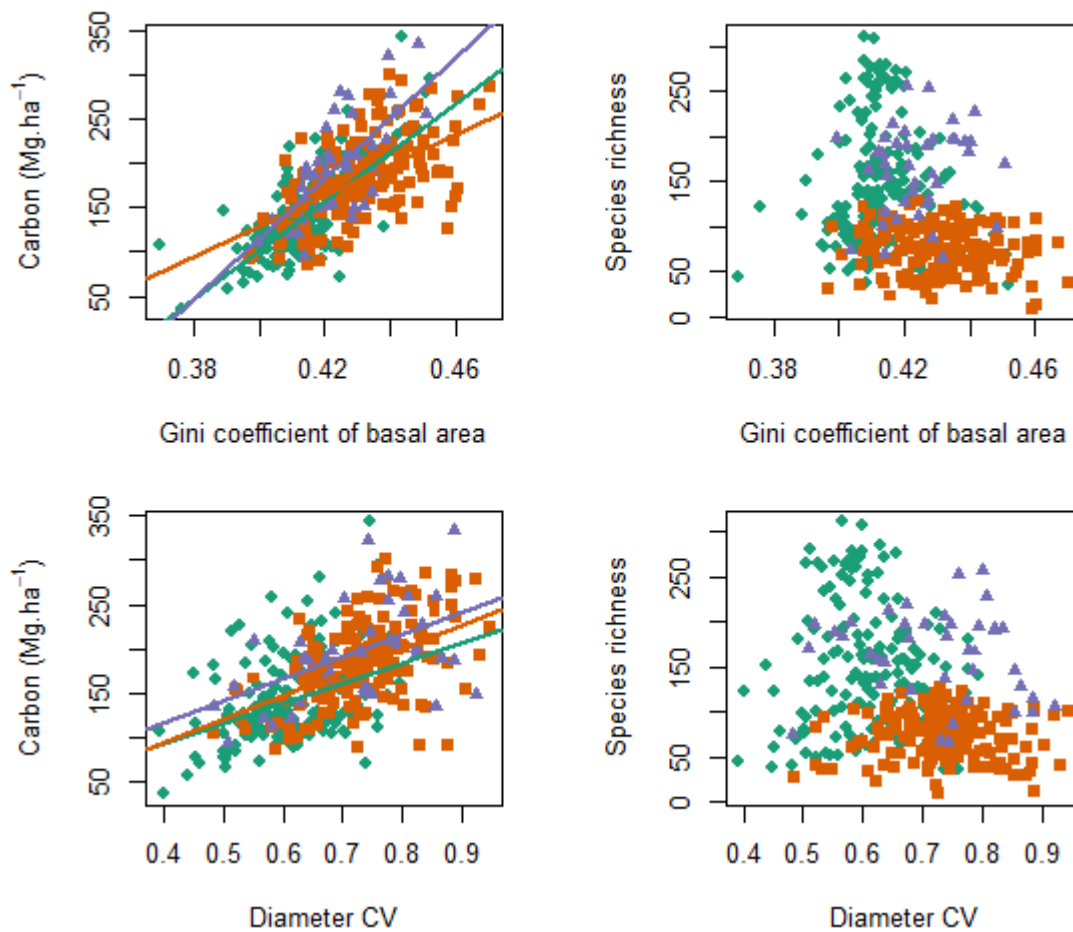
Supplementary Figure 17. Relationship between carbon storage, species richness and stem size inequality among 1 ha plots. Stem size inequality has been quantified as either the Gini coefficient of stem basal area or the coefficient of variation in stem diameters. For both metrics, higher values indicate greater inequality in stem size within a stand. In all continents, log-transformed carbon storage was positively related to both the Gini coefficient of basal area (South America: $\beta = 18.53$, $P < 0.001$; Africa: $\beta = 10.02$, $P < 0.001$; Asia: $\beta = 17.45$, $P < 0.001$) and the coefficient of variation in stem diameters (South America: $\beta = 1.74$, $P < 0.001$; Africa: $\beta = 1.49$, $P < 0.001$; Asia: $\beta = 1.37$, $P < 0.001$). There were no significant relationships between species richness and either metric of stem size inequality in any continent (negative-binomial GLM, $P \geq 0.078$).

666
667
668
669
670
671
672
673
674

675

676

677

678

679

680

681

35
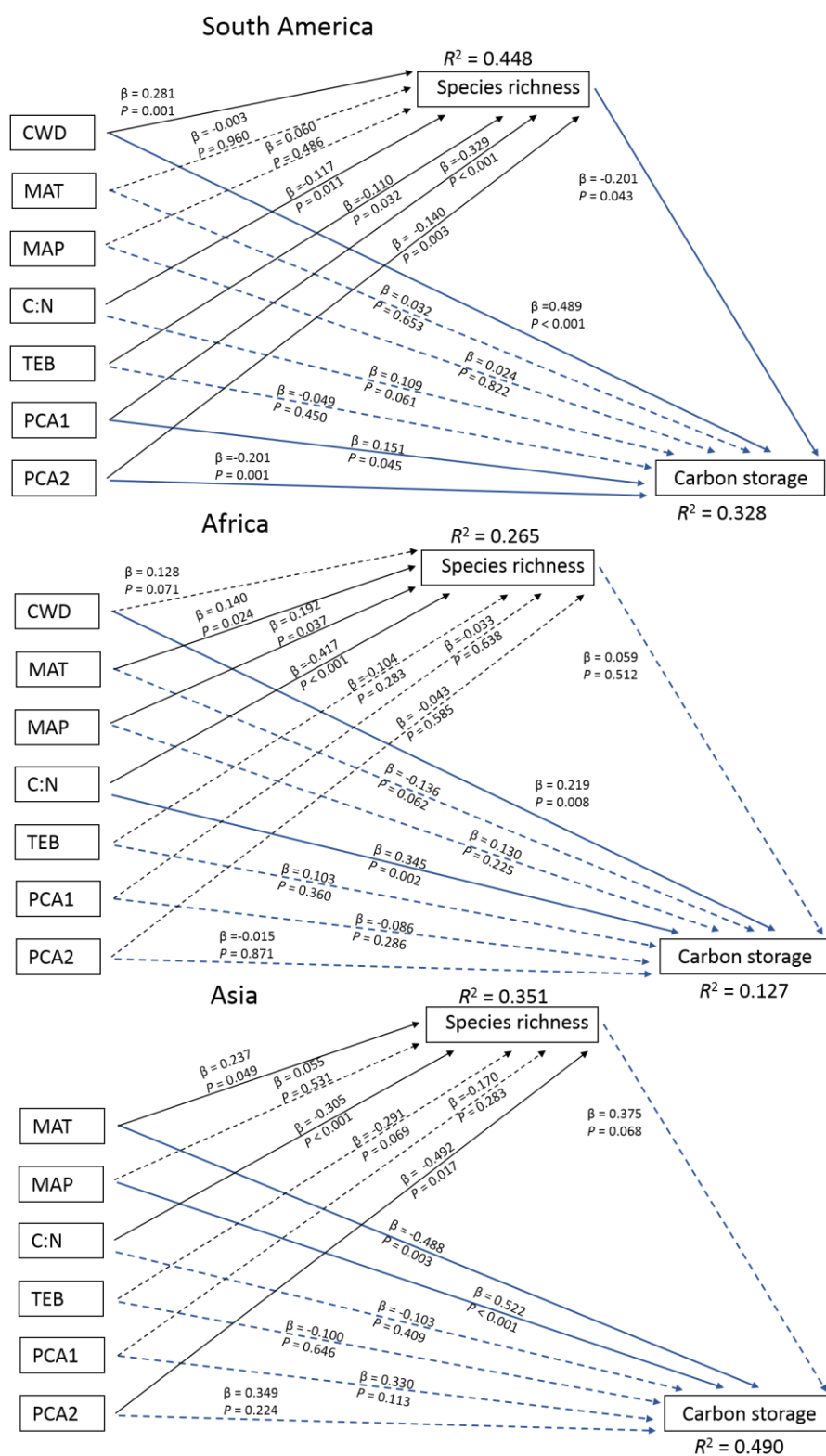
Supplementary Figure 18. Fitted structural equation models, where both species richness and carbon storage were modelled as a function of climate and soil, with carbon storage also a function of species richness. Models were parameterised separately for each continent, using the lavaan R package to define and parameterise paths. All variables were scaled and centred prior to analysis to have a mean of zero and standard deviation of one, with species richness and carbon storage also natural log transformed.

689
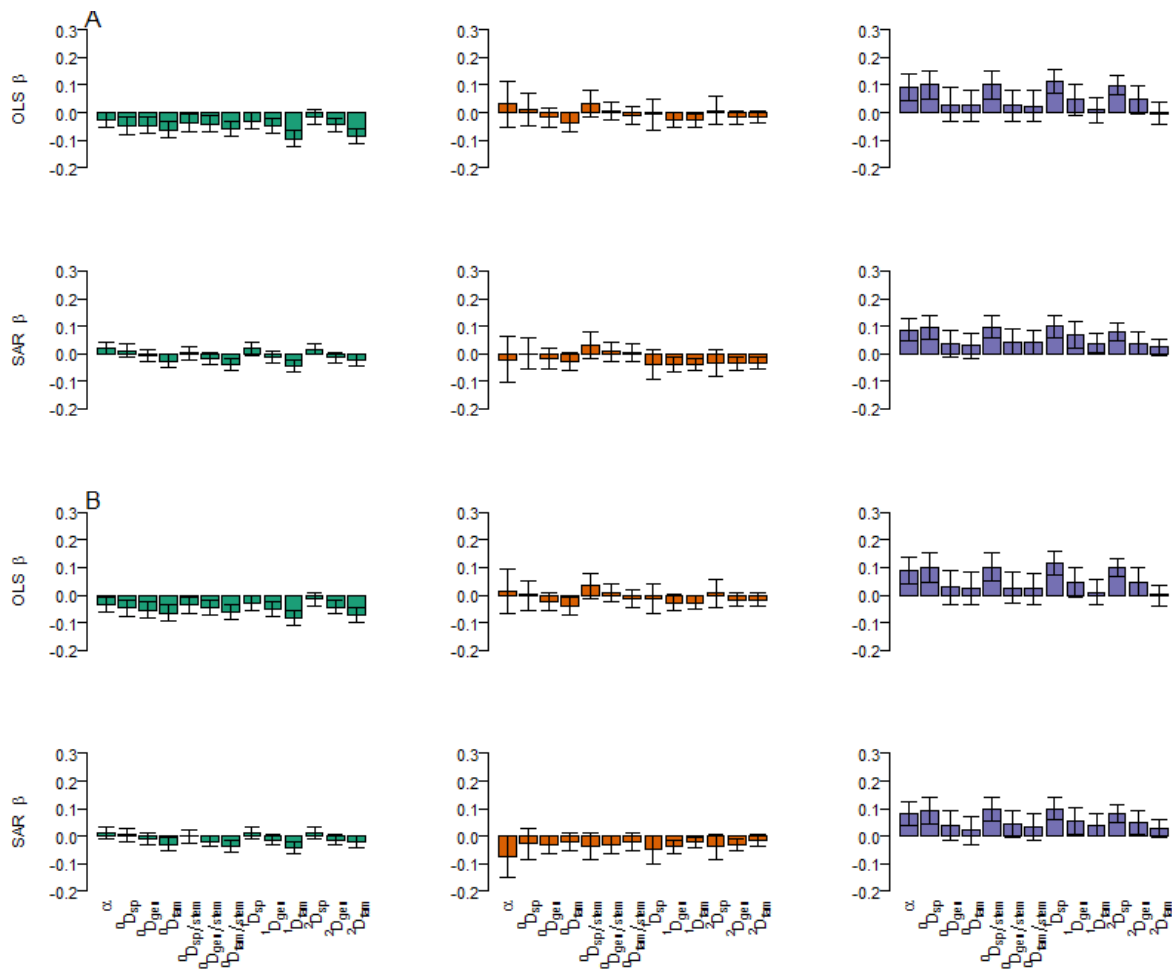
690

691

692 **Supplementary Figure 19.** Coefficients of relationships between diversity metrics and carbon
693 between 1 ha plots within continents (green = South America, orange = Africa, purple = Asia) from
694 multiple regression models also incorporating climate and edaphic variables. Results are shown for
695 models run using (a) the best estimate soil class from the Harmonised World Soil Database and (b) the
696 dominant soil class from the Harmonised World Soil Database. Diversity Hill numbers have been
697 calculated for different taxonomic levels (sp= species, gen = genus, fam = family) and by area or per
698 300 stems (taxa/ stem).

699

700

701

702

703

704

705

37

706 **Supplementary Table 1.** Loadings of first two axes of principal components analysis performed on
707 soil texture data from each 1 ha plot.

Soil texture class (%)	PC1	PC2
Sand	0.82	-0.07
Silt	-0.33	0.75
Clay	-0.47	-0.65
Proportion of variance explained	0.64	0.32

708 95.4% of variance was explained by first two axes.

709

710

711

712

713

714

715

716

717

718

719

720

721

722

723

724

725

726

727

728

729

730

731

38

732 **Supplementary Table 2.** Mean carbon storage and diversity in 1ha plots in South America, Africa
733 and Asia. 95% confidence limits derived from 10000 bootstrap resamples of the data (sampling with
734 replacement) are shown in parentheses. Different letters indicate significant differences between
735 continents (ANOVA and subsequent Tukey's all-pair comparison, $P < 0.05$).

Variable	South America	Africa	Asia
Carbon (Mg. ha^{-1})	140 (133 – 148) [A]	183 (176 – 190) [B]	197 (180 - 215) [B]
^{0}D (species level)	152 (141 – 163) [B]	74 (70 – 78) [A]	162 (147 - 177) [C]
^{0}D (genus level)	91 (86 – 96) [C]	59 (56 – 62) [A]	87 (81 - 93) [B]
^{0}D (family level)	38 (37 – 39) [B]	28 (27 – 28) [A]	40 (38 - 42) [B]
^{1}D (species level)	85 (77 – 93) [B]	37 (34 – 40) [A]	98 (86 – 110) [B]
^{1}D (genus level)	43 (41 – 46) [B]	28 (26 – 30) [A]	43 (39 – 47) [B]
^{1}D (family level)	17 (17 – 18) [B]	13 (12 – 14) [A]	19 (18 – 21) [C]
^{2}D (species level)	48 (42 – 53) [B]	22 (20 – 24) [A]	60 (51 – 70) [C]
^{2}D (genus level)	25 (23 – 26) [B]	17 (16 – 18) [A]	24 (22 – 27) [B]
^{2}D (family level)	11 (11 – 12) [B]	9 (8 – 10) [A]	12 (11 – 14) [B]
Fisher's α	80 (71 – 88) [B]	28 (26 – 30) [A]	84 (73 - 96) [B]
^{0}D (species level) / 300 stems	109 (102 – 116) [B]	65 (62 – 69) [A]	120 (111 - 130) [B]
^{0}D (genus level) / 300 stems	72 (68 – 75) [B]	54 (51 – 56) [A]	71 (66 - 75) [B]
^{0}D (family level) / 300 stems	33 (32 – 34) [B]	26 (25 – 27) [A]	35 (34 - 37) [B]

736

737

738

739

740

741

742

743

744

745

746

747

748

749

750 **Supplementary Table 3.** Mean carbon storage and tree diversity in forest inventory plots in South
751 America (n = 99), Africa (n = 105) and Asia (n = 23) where at least 90% of stems have been identified
752 to species level. 95% confidence limits derived from 10000 bootstrap resamples of the data (sampling
753 with replacement) are shown in parentheses. Different letters indicate significant differences between
754 continents (ANOVA and subsequent Tukey's all-pair comparison, $P < 0.05$). Changing the species
755 identification cut-off level for including plots has no impact on continental patterns of diversity and
756 carbon (compare to Table 1 in main manuscript).

757

Variable	South America	Africa	Asia
Carbon (Mg. ha^{-1})	133 (125 – 142) [A]	177 (168 – 187) [B]	180 (159 - 202) [B]
Fisher's α	86 (74 – 99) [B]	26 (23 – 28) [A]	83 (74 - 99) [B]
Species richness (ha^{-1})	159 (144 – 174) [B]	71 (65 – 76) [A]	161 (139 - 183) [B]
(300 stems^{-1})	111 (102 – 120) [B]	63 (59 – 67) [A]	117 (104 - 130) [B]
Genus richness (ha^{-1})	93 (87 – 99) [B]	57 (53 – 61) [A]	89 (80 - 97) [B]
(300 stems^{-1})	73 (69 – 77) [B]	53 (49 – 56) [A]	72 (69 - 77) [B]
Family richness (ha^{-1})	39 (38 – 41) [B]	27 (25 – 28) [A]	41 (38 - 43) [B]
(300 stems^{-1})	34 (33 – 35) [B]	26 (25 – 27) [A]	36 (34 - 38) [B]

758

759

760

761

762

763

764

765

766

767

768

769

770

771

772

773

40

774 **Supplementary Table 4.** Kendall's tau correlations between carbon and diversity metrics in each
775 continent. Both uncorrected *P* values and false-discovery rate corrected *P* values (*P*(fdr)) have been
776 presented. Significant relationships prior to false-discovery rate correction are shown in italics. Power
777 analysis was used to estimate the minimum effect size (presented as both τ and Pearson's *r*) detectable
778 with 80% power.

Diversity metric	South America			Africa			Asia		
	τ	P	P (fdr)	τ	P	P (fdr)	τ	P	P (fdr)
^{0}D (species level)	0.084	0.12	0.223	0.014	0.788	0.999	0.132	0.230	0.598
^{0}D (genus level)	0.066	0.223	0.362	-0.016	0.765	0.999	-0.006	0.954	0.954
^{0}D (family level)	-0.007	0.893	0.956	-0.051	0.35	0.999	0.087	0.434	0.756
^{1}D (species level)	*0.107*	*0.046*	0.223	0	0.999	0.999	*0.218*	*0.048*	0.312
^{1}D (genus level)	0.034	0.521	0.616	-0.032	0.552	0.999	0.082	0.465	0.756
^{1}D (family level)	-0.089	0.096	0.223	-0.046	0.381	0.999	0.010	0.935	0.954
^{2}D (species level)	*0.12*	*0.025*	0.223	0	0.994	0.999	*0.246*	*0.025*	0.312
^{2}D (genus level)	-0.003	0.956	0.956	-0.031	0.559	0.999	0.159	0.153	0.566
^{2}D (family level)	-0.101	0.059	0.223	-0.033	0.529	0.999	-0.028	0.808	0.954
Fischer's α	0.083	0.12	0.223	0.012	0.821	0.999	0.115	0.302	0.654
^{0}D Species/ 300 stem	0.092	0.087	0.223	0.031	0.573	0.999	0.151	0.174	0.566
^{0}D Genus/ 300 stem	0.059	0.272	0.393	0.01	0.859	0.999	-0.051	0.652	0.942
^{0}D Family/ 300 stem	-0.042	0.43	0.559	-0.036	0.519	0.999	0.021	0.862	0.954
Detectable effect size	τ = 0.14 r = 0.22			τ = 0.14 r = 0.22			τ = 0.28 r = 0.43		

779

780

781

782

783

784

785

786

787

41

788 **Supplementary Table 5** Averaged multiple regression model for ln(carbon) in 1 ha plots as a
789 function of species richness, climate and soil variables. Both non-spatial ordinary least squares (OLS)
790 and spatial simultaneous autoregressive error (SAR) models have been shown. $\sum\omega_i$ is the sum of AIC_C
791 weights in models containing a variable, with values close to 1 indicating strong support for a
792 variable.

Variable	OLS					SAR				
	β	SE	Z	P	$\sum\omega_i$	β	SE	Z	P	$\sum\omega_i$
South America Fisher's α										
(Intercept)	4.931	0.028	176.801	0.000	NA	4.838	0.113	42.778	0.000	NA
C:N ratio	0.050	0.025	2.033	0.042	0.77	0.007	0.018	0.406	0.685	0.26
CWD	0.163	0.030	5.408	0.000	1.00	0.101	0.034	2.994	0.003	0.98
Fisher's α	-0.026	0.029	0.899	0.369	0.35	0.019	0.022	0.886	0.376	0.32
MAP	-0.018	0.034	0.522	0.602	0.27	0.005	0.035	0.150	0.881	0.29
MAT	0.030	0.025	1.187	0.235	0.41	-0.009	0.021	0.441	0.659	0.26
PCA1	0.086	0.026	3.330	0.001	1.00	0.004	0.021	0.175	0.861	0.24
PCA2	-0.041	0.019	2.146	0.032	0.81	-0.025	0.017	1.461	0.144	0.48
TEB	-0.009	0.021	0.423	0.672	0.27	0.034	0.015	2.194	0.028	0.80
Africa Fisher's α										
(Intercept)	5.195	0.040	129.606	0.000	NA	5.182	0.063	82.417	0.000	NA
C:N ratio	-0.016	0.038	0.426	0.670	0.28	-0.036	0.043	0.818	0.414	0.31
CWD	0.062	0.028	2.194	0.028	0.81	0.099	0.031	3.200	0.001	1.00
Fisher's α	0.031	0.084	0.365	0.715	0.26	-0.022	0.083	0.260	0.795	0.24
MAP	0.065	0.047	1.365	0.172	0.51	-0.032	0.046	0.684	0.494	0.28
MAT	-0.031	0.026	1.194	0.232	0.41	0.034	0.028	1.200	0.230	0.39
PCA1	0.029	0.030	0.944	0.345	0.35	0.034	0.034	0.985	0.325	0.35
PCA2	-0.007	0.039	0.191	0.849	0.25	-0.038	0.043	0.880	0.379	0.32
TEB	-0.070	0.047	1.491	0.136	0.56	-0.011	0.046	0.247	0.805	0.25
Asia Fisher's α										
(Intercept)	5.073	0.068	72.799	0.000	NA	5.113	0.125	41.019	0.000	NA
C:N ratio	0.015	0.024	0.598	0.550	0.07	0.002	0.020	0.089	0.929	0.06
Fisher's α	0.090	0.049	1.778	0.075	0.42	0.086	0.041	2.118	0.034	0.50
MAP	0.179	0.041	4.222	0.000	1.00	0.128	0.038	3.408	0.001	1.00
MAT	-0.118	0.055	2.083	0.037	0.64	-0.105	0.045	2.303	0.021	0.60
PCA1	-0.025	0.069	0.347	0.729	0.08	-0.032	0.056	0.564	0.573	0.07
PCA2	0.030	0.151	0.194	0.846	0.06	-0.017	0.151	0.110	0.912	0.07
TEB	0.197	0.237	0.804	0.422	0.10	0.258	0.207	1.247	0.212	0.14
South America Species richness										
(Intercept)	4.936	0.029	169.527	0.000	NA	4.838	0.113	42.930	0.000	NA
C:N ratio	0.049	0.025	1.949	0.051	0.73	0.007	0.018	0.399	0.690	0.26
CWD	0.168	0.031	5.344	0.000	1.00	0.102	0.034	2.997	0.003	0.98
MAP	-0.018	0.034	0.522	0.602	0.26	0.006	0.034	0.188	0.851	0.29
MAT	0.030	0.025	1.185	0.236	0.40	-0.009	0.021	0.427	0.670	0.25
PCA1	0.080	0.027	2.918	0.004	0.97	0.002	0.020	0.116	0.908	0.24
PCA2	-0.044	0.020	2.233	0.026	0.85	-0.025	0.017	1.450	0.147	0.48
Species richness	-0.047	0.033	1.409	0.159	0.50	0.012	0.025	0.487	0.626	0.26
TEB	-0.011	0.021	0.517	0.605	0.28	0.033	0.015	2.177	0.029	0.79
Africa Species richness										
(Intercept)	5.192	0.035	148.990	0.000	NA	5.185	0.060	85.967	0.000	NA
C:N ratio	-0.017	0.038	0.446	0.655	0.28	-0.034	0.043	0.796	0.426	0.31
CWD	0.062	0.028	2.211	0.027	0.81	0.099	0.031	3.195	0.001	1.00
MAP	0.064	0.047	1.357	0.175	0.50	-0.032	0.046	0.684	0.494	0.28
MAT	-0.031	0.026	1.190	0.234	0.41	0.034	0.028	1.192	0.233	0.39

PCA1	0.029	0.030	0.945	0.344	0.35	0.033	0.034	0.975	0.330	0.35
PCA2	-0.007	0.039	0.183	0.855	0.25	-0.038	0.043	0.890	0.373	0.32
Species richness	0.010	0.057	0.177	0.859	0.25	0.001	0.057	0.017	0.987	0.23
TEB	-0.069	0.047	1.482	0.138	0.55	-0.012	0.046	0.250	0.802	0.25
Asia Species richness										
(Intercept)	5.069	0.069	71.481	0.000	NA	5.109	0.123	41.417	0.000	NA
C:N ratio	0.015	0.024	0.598	0.550	0.07	0.002	0.020	0.124	0.901	0.05
MAP	0.179	0.041	4.238	0.000	1.00	0.128	0.037	3.436	0.001	1.00
MAT	-0.122	0.055	2.135	0.033	0.67	-0.110	0.046	2.380	0.017	0.65
PCA1	-0.026	0.069	0.359	0.719	0.08	-0.033	0.057	0.585	0.558	0.07
PCA2	0.022	0.150	0.141	0.888	0.06	-0.017	0.151	0.114	0.909	0.06
Species richness	0.100	0.052	1.852	0.064	0.44	0.096	0.044	2.190	0.029	0.53
TEB	0.193	0.236	0.791	0.429	0.10	0.253	0.207	1.224	0.221	0.12
South America Genus richness										
(Intercept)	4.937	0.029	169.730	0.000	NA	4.841	0.112	43.148	0.000	NA
C:N ratio	0.051	0.024	2.065	0.039	0.78	0.007	0.018	0.399	0.690	0.25
CWD	0.167	0.030	5.518	0.000	1.00	0.103	0.034	3.023	0.002	0.98
Genus richness	-0.046	0.030	1.501	0.133	0.53	-0.007	0.022	0.324	0.746	0.25
MAP	-0.016	0.034	0.464	0.642	0.26	0.008	0.034	0.243	0.808	0.29
MAT	0.028	0.025	1.098	0.272	0.38	-0.010	0.021	0.450	0.653	0.26
PCA1	0.080	0.027	2.932	0.003	0.98	0.000	0.020	0.006	0.995	0.24
PCA2	-0.041	0.019	2.178	0.029	0.82	-0.025	0.017	1.440	0.150	0.48
TEB	-0.010	0.021	0.491	0.624	0.27	0.033	0.015	2.159	0.031	0.78
Africa Genus richness										
(Intercept)	5.188	0.031	164.165	0.000	NA	5.182	0.059	88.360	0.000	NA
C:N ratio	-0.019	0.038	0.496	0.620	0.29	-0.037	0.044	0.838	0.402	0.32
CWD	0.063	0.028	2.252	0.024	0.82	0.099	0.031	3.207	0.001	1.00
Genus richness	-0.017	0.035	0.475	0.635	0.27	-0.018	0.036	0.503	0.615	0.26
MAP	0.064	0.047	1.346	0.178	0.50	-0.031	0.046	0.679	0.497	0.28
MAT	-0.030	0.026	1.180	0.238	0.41	0.034	0.028	1.200	0.230	0.39
PCA1	0.028	0.030	0.929	0.353	0.34	0.034	0.034	0.995	0.320	0.35
PCA2	-0.006	0.039	0.147	0.883	0.25	-0.037	0.043	0.868	0.385	0.31
TEB	-0.068	0.047	1.448	0.148	0.54	-0.011	0.046	0.238	0.812	0.25
Asia Genus richness										
(Intercept)	5.092	0.064	77.681	0.000	NA	5.222	0.145	36.096	0.000	NA
C:N ratio	0.014	0.024	0.578	0.563	0.12	-0.010	0.021	0.464	0.642	0.08
Genus richness	0.028	0.061	0.452	0.651	0.10	0.037	0.048	0.785	0.432	0.09
MAP	0.176	0.041	4.119	0.000	1.00	0.081	0.036	2.280	0.023	0.51
MAT	-0.111	0.055	1.953	0.051	0.61	-0.104	0.041	2.537	0.011	0.71
PCA1	-0.019	0.069	0.272	0.785	0.09	-0.108	0.082	1.324	0.186	0.23
PCA2	0.010	0.163	0.058	0.954	0.10	-0.355	0.249	1.424	0.154	0.28
TEB	0.189	0.246	0.745	0.456	0.14	0.561	0.339	1.652	0.099	0.40
South America Family richness										
(Intercept)	4.948	0.030	163.808	0.000	NA	4.845	0.112	43.193	0.000	NA
C:N ratio	0.050	0.024	2.062	0.039	0.78	0.007	0.018	0.395	0.693	0.25
CWD	0.168	0.028	5.925	0.000	1.00	0.103	0.034	3.009	0.003	0.98
Family richness	-0.064	0.030	2.133	0.033	0.80	-0.026	0.022	1.178	0.239	0.40
MAP	-0.010	0.034	0.292	0.770	0.25	0.011	0.034	0.332	0.740	0.30
MAT	0.022	0.025	0.864	0.387	0.32	-0.012	0.022	0.554	0.579	0.27

PCA1	0.073	0.026	2.757	0.006	0.97	-0.003	0.021	0.160	0.873	0.25
PCA2	-0.041	0.018	2.184	0.029	0.82	-0.025	0.017	1.435	0.151	0.47
TEB	-0.011	0.020	0.520	0.603	0.27	0.033	0.015	2.153	0.031	0.77
Africa Family richness										
(Intercept)	5.182	0.033	154.128	0.000	NA	5.179	0.059	87.131	0.000	NA
C:N ratio	-0.020	0.038	0.537	0.591	0.29	-0.038	0.044	0.870	0.384	0.32
CWD	0.065	0.028	2.310	0.021	0.84	0.100	0.031	3.221	0.001	1.00
Family richness	-0.036	0.034	1.042	0.297	0.36	-0.027	0.033	0.816	0.414	0.31
MAP	0.063	0.047	1.343	0.179	0.50	-0.031	0.046	0.660	0.509	0.28
MAT	-0.030	0.026	1.162	0.245	0.40	0.033	0.028	1.180	0.238	0.38
PCA1	0.027	0.030	0.891	0.373	0.33	0.035	0.034	1.010	0.313	0.36
PCA2	-0.004	0.039	0.092	0.927	0.25	-0.036	0.043	0.844	0.399	0.31
TEB	-0.066	0.048	1.383	0.167	0.51	-0.011	0.046	0.228	0.820	0.24
Asia Family richness										
(Intercept)	5.092	0.064	76.789	0.000	NA	5.222	0.145	36.041	0.000	NA
C:N ratio	0.014	0.024	0.578	0.563	0.12	-0.010	0.021	0.478	0.633	0.09
Family richness	0.024	0.059	0.399	0.690	0.10	0.030	0.045	0.673	0.501	0.08
MAP	0.176	0.041	4.124	0.000	1.00	0.081	0.036	2.261	0.024	0.50
MAT	-0.111	0.055	1.950	0.051	0.61	-0.103	0.041	2.532	0.011	0.71
PCA1	-0.019	0.069	0.272	0.785	0.09	-0.108	0.082	1.320	0.187	0.23
PCA2	0.010	0.163	0.058	0.954	0.10	-0.355	0.249	1.424	0.155	0.28
TEB	0.189	0.246	0.745	0.456	0.14	0.560	0.340	1.648	0.099	0.40
South America Species per 300 stems										
(Intercept)	4.933	0.028	174.606	0.000	NA	4.845	0.109	44.318	0.000	NA
C:N ratio	0.049	0.025	1.997	0.046	0.74	0.007	0.018	0.391	0.696	0.26
CWD	0.165	0.031	5.324	0.000	1.00	0.097	0.033	2.916	0.004	0.97
MAP	-0.015	0.039	0.370	0.711	0.26	0.005	0.035	0.129	0.897	0.27
MAT	0.030	0.025	1.199	0.231	0.42	-0.012	0.022	0.554	0.580	0.27
PCA1	0.083	0.026	3.123	0.002	1.00	0.002	0.020	0.076	0.940	0.24
PCA2	-0.043	0.019	2.194	0.028	0.83	-0.023	0.017	1.321	0.187	0.44
Species per 300 stems	-0.038	0.031	1.202	0.229	0.42	0.004	0.024	0.154	0.877	0.24
TEB	-0.007	0.024	0.286	0.775	0.26	0.030	0.017	1.788	0.074	0.62
Africa Species per 300 stems										
(Intercept)	5.206	0.037	138.288	0.000	NA	5.197	0.066	79.307	0.000	NA
C:N ratio	-0.051	0.040	1.264	0.206	0.43	-0.043	0.045	0.962	0.336	0.34
CWD	0.010	0.043	0.225	0.822	0.31	0.076	0.037	2.076	0.038	0.76
MAP	0.092	0.043	2.098	0.036	0.78	-0.030	0.050	0.590	0.555	0.27
MAT	-0.009	0.028	0.320	0.749	0.26	0.048	0.030	1.585	0.113	0.52
PCA1	0.029	0.033	0.885	0.376	0.34	0.028	0.034	0.834	0.404	0.31
PCA2	0.020	0.043	0.462	0.644	0.27	-0.018	0.044	0.406	0.685	0.25
Species per 300 stems	0.033	0.047	0.690	0.490	0.30	0.033	0.048	0.690	0.490	0.28
TEB	-0.103	0.044	2.332	0.020	0.90	-0.014	0.055	0.256	0.798	0.26
Asia Species per 300 stems										
(Intercept)	5.054	0.076	64.759	0.000	NA	5.093	0.127	40.034	0.000	NA
C:N ratio	0.015	0.023	0.622	0.534	0.07	0.003	0.020	0.130	0.896	0.05
MAP	0.181	0.041	4.282	0.000	1.00	0.130	0.037	3.486	0.000	1.00
MAT	-0.117	0.054	2.103	0.035	0.63	-0.104	0.044	2.346	0.019	0.60
PCA1	-0.027	0.069	0.381	0.703	0.08	-0.035	0.056	0.624	0.533	0.07
PCA2	0.037	0.150	0.237	0.813	0.04	0.014	0.127	0.113	0.910	0.05
Species per 300 stems	0.101	0.050	1.941	0.052	0.53	0.097	0.042	2.333	0.020	0.60

TEB	0.201	0.236	0.823	0.411	0.10	0.253	0.194	1.305	0.192	0.12
South America Genera per 300 stems										
(Intercept)	4.933	0.028	176.185	0.000	NA	4.846	0.109	44.414	0.000	NA
C:N ratio	0.051	0.024	2.058	0.040	0.78	0.007	0.018	0.398	0.690	0.25
CWD	0.165	0.030	5.473	0.000	1.00	0.098	0.033	2.943	0.003	0.97
Genera per 300 stems	-0.041	0.028	1.447	0.148	0.50	-0.016	0.021	0.786	0.432	0.30
MAP	-0.012	0.039	0.311	0.756	0.25	0.006	0.035	0.175	0.861	0.27
MAT	0.028	0.025	1.123	0.261	0.39	-0.013	0.022	0.591	0.554	0.27
PCA1	0.081	0.027	3.003	0.003	0.99	-0.001	0.021	0.067	0.946	0.24
PCA2	-0.041	0.019	2.173	0.030	0.82	-0.023	0.017	1.311	0.190	0.44
TEB	-0.007	0.024	0.292	0.770	0.26	0.029	0.017	1.765	0.078	0.61
Africa Genera per 300 stems										
(Intercept)	5.202	0.034	152.373	0.000	NA	5.192	0.064	81.491	0.000	NA
C:N ratio	-0.053	0.040	1.315	0.189	0.45	-0.045	0.045	0.996	0.319	0.35
CWD	0.010	0.043	0.236	0.813	0.31	0.076	0.037	2.078	0.038	0.77
Genera per 300 stems	0.008	0.032	0.239	0.811	0.25	0.008	0.033	0.237	0.813	0.24
MAP	0.093	0.043	2.127	0.033	0.78	-0.029	0.050	0.572	0.568	0.27
MAT	-0.008	0.028	0.270	0.787	0.26	0.048	0.030	1.606	0.108	0.53
PCA1	0.029	0.033	0.892	0.372	0.34	0.029	0.034	0.856	0.392	0.32
PCA2	0.022	0.043	0.503	0.615	0.28	-0.016	0.044	0.379	0.705	0.24
TEB	-0.104	0.044	2.346	0.019	0.91	-0.014	0.055	0.257	0.797	0.26
Asia Genera per 300 stems										
(Intercept)	5.092	0.064	77.413	0.000	NA	5.221	0.145	36.130	0.000	NA
C:N ratio	0.015	0.024	0.598	0.550	0.11	-0.010	0.021	0.490	0.624	0.09
Genera per 300 stems	0.025	0.057	0.427	0.669	0.11	0.044	0.046	0.966	0.334	0.10
MAP	0.176	0.041	4.116	0.000	1.00	0.081	0.035	2.282	0.023	0.51
MAT	-0.111	0.055	1.950	0.051	0.61	-0.104	0.041	2.540	0.011	0.71
PCA1	-0.019	0.069	0.272	0.785	0.09	-0.108	0.082	1.322	0.186	0.22
PCA2	0.010	0.163	0.058	0.954	0.10	-0.355	0.249	1.425	0.154	0.27
TEB	0.189	0.246	0.746	0.456	0.14	0.560	0.339	1.650	0.099	0.39
South America Families per 300 stems										
(Intercept)	4.940	0.028	175.164	0.000	NA	4.851	0.110	44.195	0.000	NA
C:N ratio	0.050	0.024	2.062	0.039	0.77	0.007	0.018	0.396	0.692	0.25
CWD	0.163	0.028	5.734	0.000	1.00	0.096	0.034	2.850	0.004	0.95
Families per 300 stems	-0.060	0.027	2.182	0.029	0.81	-0.038	0.021	1.798	0.072	0.65
MAP	-0.002	0.040	0.057	0.955	0.24	0.018	0.037	0.497	0.620	0.31
MAT	0.023	0.025	0.913	0.362	0.34	-0.018	0.022	0.812	0.417	0.31
PCA1	0.072	0.026	2.713	0.007	0.97	-0.011	0.023	0.488	0.625	0.28
PCA2	-0.041	0.019	2.192	0.028	0.82	-0.023	0.017	1.307	0.191	0.43
TEB	-0.006	0.023	0.244	0.807	0.25	0.029	0.017	1.759	0.079	0.61
Africa Families per 300 stems										
(Intercept)	5.199	0.034	151.668	0.000	NA	5.192	0.064	81.181	0.000	NA
C:N ratio	-0.055	0.040	1.362	0.173	0.47	-0.045	0.045	1.001	0.317	0.35
CWD	0.011	0.043	0.251	0.802	0.31	0.076	0.037	2.083	0.037	0.77
Families per 300 stems	-0.010	0.033	0.304	0.761	0.25	0.004	0.033	0.137	0.891	0.23
MAP	0.093	0.043	2.136	0.033	0.79	-0.029	0.050	0.578	0.563	0.27
MAT	-0.006	0.028	0.223	0.824	0.25	0.048	0.030	1.614	0.106	0.54
PCA1	0.029	0.033	0.890	0.373	0.34	0.029	0.034	0.862	0.389	0.32
PCA2	0.023	0.043	0.539	0.590	0.28	-0.016	0.044	0.375	0.708	0.25
TEB	-0.105	0.044	2.355	0.019	0.91	-0.014	0.056	0.254	0.800	0.26

Asia Families per 300 stems									
(Intercept)	5.092	0.065	76.189	0.000	NA	5.219	0.145	35.990	0.000	NA
C:N ratio	0.015	0.024	0.598	0.550	0.11	-0.009	0.020	0.449	0.654	0.08
Families per 300 stems	0.023	0.056	0.394	0.694	0.10	0.044	0.043	1.028	0.304	0.13
MAP	0.176	0.041	4.123	0.000	1.00	0.080	0.036	2.264	0.024	0.48
MAT	-0.110	0.055	1.948	0.051	0.60	-0.103	0.041	2.532	0.011	0.71
PCA1	-0.019	0.069	0.272	0.785	0.09	-0.107	0.081	1.315	0.189	0.23
PCA2	0.010	0.163	0.058	0.954	0.10	-0.360	0.248	1.449	0.147	0.26
TEB	0.189	0.246	0.746	0.456	0.14	0.556	0.339	1.638	0.101	0.39
South America Shannon index_sp									
(Intercept)	4.932	0.028	176.548	0.000	NA	4.838	0.113	42.840	0.000	NA
C:N ratio	0.050	0.025	2.017	0.044	0.76	0.007	0.018	0.409	0.682	0.26
CWD	0.165	0.030	5.372	0.000	1.00	0.102	0.034	3.001	0.003	0.98
Shannon index_sp	-0.030	0.029	1.030	0.303	0.38	0.018	0.023	0.786	0.432	0.30
MAP	-0.018	0.034	0.534	0.593	0.27	0.006	0.034	0.172	0.864	0.29
MAT	0.029	0.025	1.167	0.243	0.40	-0.009	0.021	0.420	0.674	0.25
PCA1	0.085	0.025	3.317	0.001	1.00	0.003	0.021	0.154	0.878	0.24
PCA2	-0.042	0.019	2.163	0.031	0.83	-0.025	0.017	1.446	0.148	0.48
TEB	-0.009	0.021	0.427	0.669	0.26	0.033	0.015	2.190	0.029	0.80
Africa Shannon index_sp									
(Intercept)	5.189	0.033	154.343	0.000	NA	5.179	0.061	84.831	0.000	NA
C:N ratio	-0.018	0.038	0.467	0.640	0.28	-0.037	0.044	0.850	0.395	0.32
CWD	0.063	0.028	2.230	0.026	0.82	0.099	0.031	3.207	0.001	1.00
Shannon index_sp	-0.007	0.055	0.118	0.906	0.24	-0.037	0.053	0.700	0.484	0.29
MAP	0.064	0.047	1.355	0.175	0.51	-0.031	0.046	0.664	0.507	0.28
MAT	-0.031	0.026	1.188	0.235	0.41	0.034	0.028	1.202	0.229	0.39
PCA1	0.029	0.030	0.946	0.344	0.35	0.035	0.035	1.017	0.309	0.36
PCA2	-0.007	0.039	0.168	0.866	0.25	-0.037	0.043	0.851	0.395	0.31
TEB	-0.069	0.047	1.471	0.141	0.55	-0.011	0.046	0.243	0.808	0.25
Asia Shannon index_sp									
(Intercept)	5.038	0.067	72.796	0.000	NA	5.169	0.129	40.203	0.000	NA
C:N ratio	0.013	0.023	0.567	0.571	0.03	-0.007	0.020	0.375	0.707	0.03
Shannon index_sp	0.114	0.044	2.528	0.011	0.83	0.099	0.039	2.525	0.012	0.64
MAP	0.183	0.039	4.524	0.000	1.00	0.089	0.033	2.710	0.007	0.64
MAT	-0.132	0.052	2.433	0.015	0.76	-0.117	0.040	2.921	0.003	0.84
PCA1	-0.039	0.070	0.541	0.589	0.04	-0.102	0.078	1.299	0.194	0.12
PCA2	0.055	0.150	0.355	0.723	0.03	-0.351	0.257	1.365	0.172	0.11
TEB	0.228	0.231	0.956	0.339	0.05	0.504	0.322	1.567	0.117	0.22
South America Shannon index_gen									
(Intercept)	4.937	0.028	175.385	0.000	NA	4.841	0.112	43.232	0.000	NA
C:N ratio	0.050	0.024	2.068	0.039	0.78	0.007	0.018	0.395	0.693	0.26
CWD	0.170	0.029	5.718	0.000	1.00	0.102	0.034	3.021	0.003	0.98
Shannon index_gen	-0.049	0.026	1.835	0.067	0.66	-0.012	0.020	0.627	0.531	0.28
MAP	-0.013	0.034	0.392	0.695	0.26	0.009	0.034	0.249	0.803	0.29
MAT	0.024	0.025	0.961	0.337	0.34	-0.010	0.022	0.478	0.633	0.26
PCA1	0.078	0.026	2.930	0.003	0.99	0.000	0.020	0.020	0.984	0.24
PCA2	-0.041	0.019	2.189	0.029	0.83	-0.025	0.017	1.442	0.149	0.48
TEB	-0.008	0.021	0.390	0.697	0.26	0.033	0.015	2.160	0.031	0.78
Africa Shannon index_gen									
(Intercept)	5.186	0.031	165.462	0.000	NA	5.174	0.060	86.411	0.000	NA

C:N ratio	-0.021	0.038	0.538	0.590	0.29	-0.042	0.044	0.952	0.341	0.35
CWD	0.063	0.028	2.264	0.024	0.83	0.100	0.031	3.238	0.001	1.00
Shannon index_gen	-0.027	0.029	0.933	0.351	0.34	-0.040	0.028	1.437	0.151	0.49
MAP	0.063	0.047	1.341	0.180	0.50	-0.031	0.046	0.665	0.506	0.27
MAT	-0.030	0.026	1.169	0.242	0.40	0.035	0.028	1.233	0.218	0.40
PCA1	0.029	0.030	0.944	0.345	0.35	0.039	0.035	1.117	0.264	0.38
PCA2	-0.004	0.039	0.095	0.925	0.25	-0.033	0.044	0.751	0.453	0.30
TEB	-0.068	0.047	1.447	0.148	0.54	-0.012	0.046	0.250	0.803	0.24
Asia Shannon index_gen										
(Intercept)	5.092	0.063	77.850	0.000	NA	5.236	0.083	62.925	0.000	NA
C:N ratio	0.015	0.024	0.598	0.550	0.11	-0.023	0.020	1.145	0.252	0.20
Shannon index_gen	0.046	0.055	0.805	0.421	0.13	0.070	0.048	1.478	0.139	0.29
MAP	0.176	0.041	4.129	0.000	1.00	0.093	0.047	1.966	0.049	0.41
MAT	-0.111	0.055	1.960	0.050	0.61	-0.104	0.050	2.062	0.039	0.58
PCA1	-0.019	0.069	0.272	0.785	0.09	-0.058	0.088	0.665	0.506	0.15
PCA2	0.010	0.163	0.058	0.954	0.09	-0.161	0.208	0.773	0.440	0.17
TEB	0.189	0.245	0.744	0.457	0.13	0.293	0.315	0.930	0.352	0.18
South America Shannon index_fam										
(Intercept)	4.944	0.027	184.020	0.000	NA	4.847	0.110	44.008	0.000	NA
C:N ratio	0.038	0.024	1.579	0.114	0.56	0.004	0.018	0.241	0.809	0.24
CWD	0.166	0.026	6.221	0.000	1.00	0.097	0.034	2.824	0.005	0.95
Shannon index_fam	-0.095	0.028	3.319	0.001	1.00	-0.042	0.022	1.933	0.053	0.71
MAP	-0.002	0.034	0.048	0.961	0.24	0.021	0.036	0.585	0.559	0.33
MAT	0.008	0.025	0.304	0.761	0.24	-0.021	0.023	0.926	0.355	0.34
PCA1	0.059	0.024	2.373	0.018	0.89	-0.010	0.022	0.472	0.637	0.27
PCA2	-0.044	0.018	2.453	0.014	0.90	-0.024	0.017	1.389	0.165	0.46
TEB	-0.004	0.020	0.177	0.859	0.25	0.033	0.015	2.155	0.031	0.77
Africa Shannon index_fam										
(Intercept)	5.186	0.031	168.170	0.000	NA	5.169	0.061	85.173	0.000	NA
C:N ratio	-0.019	0.038	0.492	0.623	0.28	-0.048	0.045	1.063	0.288	0.37
CWD	0.063	0.028	2.258	0.024	0.83	0.101	0.031	3.278	0.001	1.00
Shannon index_fam	-0.028	0.024	1.137	0.256	0.39	-0.040	0.023	1.781	0.075	0.63
MAP	0.066	0.047	1.390	0.165	0.52	-0.023	0.047	0.494	0.621	0.26
MAT	-0.030	0.026	1.167	0.243	0.40	0.031	0.028	1.101	0.271	0.37
PCA1	0.030	0.030	0.977	0.328	0.36	0.046	0.036	1.282	0.200	0.44
PCA2	-0.002	0.040	0.058	0.954	0.25	-0.026	0.045	0.586	0.558	0.27
TEB	-0.068	0.047	1.436	0.151	0.54	-0.010	0.046	0.208	0.835	0.24
Asia Shannon index_fam										
(Intercept)	5.093	0.064	77.150	0.000	NA	5.219	0.144	36.124	0.000	NA
C:N ratio	0.014	0.024	0.578	0.563	0.12	-0.010	0.021	0.476	0.634	0.08
Shannon index_fam	0.009	0.047	0.187	0.852	0.09	0.039	0.035	1.128	0.259	0.15
MAP	0.175	0.041	4.121	0.000	1.00	0.080	0.036	2.227	0.026	0.47
MAT	-0.110	0.055	1.942	0.052	0.60	-0.102	0.041	2.485	0.013	0.70
PCA1	-0.019	0.069	0.272	0.785	0.10	-0.106	0.081	1.301	0.193	0.22
PCA2	0.010	0.163	0.058	0.954	0.10	-0.350	0.252	1.389	0.165	0.26
TEB	0.189	0.246	0.745	0.456	0.14	0.552	0.341	1.618	0.106	0.38
South America Simpson index_sp										
(Intercept)	4.930	0.027	179.125	0.000	NA	4.839	0.113	42.939	0.000	NA
C:N ratio	0.051	0.024	2.068	0.039	0.78	0.007	0.018	0.409	0.683	0.26
CWD	0.162	0.029	5.456	0.000	1.00	0.102	0.034	3.015	0.003	0.98

Simpson index_sp	-0.017	0.027	0.632	0.528	0.29	0.016	0.020	0.800	0.424	0.30
MAP	-0.018	0.034	0.532	0.595	0.26	0.006	0.034	0.179	0.858	0.29
MAT	0.029	0.025	1.150	0.250	0.39	-0.009	0.021	0.422	0.673	0.25
PCA1	0.088	0.024	3.598	0.000	1.00	0.003	0.020	0.135	0.892	0.24
PCA2	-0.040	0.019	2.120	0.034	0.80	-0.025	0.017	1.444	0.149	0.48
TEB	-0.008	0.021	0.392	0.695	0.26	0.033	0.015	2.189	0.029	0.79
Africa Simpson index_sp										
(Intercept)	5.191	0.032	160.645	0.000	NA	5.180	0.060	86.548	0.000	NA
C:N ratio	-0.017	0.038	0.450	0.653	0.28	-0.037	0.044	0.847	0.397	0.32
CWD	0.062	0.028	2.227	0.026	0.82	0.099	0.031	3.203	0.001	1.00
Simpson index_sp	0.007	0.051	0.139	0.890	0.24	-0.033	0.048	0.698	0.485	0.29
MAP	0.064	0.047	1.352	0.177	0.51	-0.031	0.046	0.667	0.505	0.28
MAT	-0.031	0.026	1.191	0.234	0.41	0.034	0.028	1.197	0.231	0.39
PCA1	0.029	0.030	0.943	0.346	0.35	0.035	0.035	1.021	0.307	0.36
PCA2	-0.007	0.039	0.184	0.854	0.25	-0.037	0.043	0.853	0.394	0.31
TEB	-0.069	0.047	1.471	0.141	0.55	-0.012	0.046	0.252	0.801	0.25
Asia Simpson index_sp										
(Intercept)	5.041	0.060	81.465	0.000	NA	5.180	0.124	41.909	0.000	NA
C:N ratio	0.009	0.024	0.378	0.705	0.02	-0.012	0.020	0.576	0.565	0.05
Simpson index_sp	0.099	0.034	2.812	0.005	0.92	0.079	0.030	2.620	0.009	0.71
MAP	0.181	0.038	4.594	0.000	1.00	0.084	0.032	2.591	0.010	0.56
MAT	-0.136	0.050	2.610	0.009	0.78	-0.117	0.040	2.924	0.003	0.84
PCA1	-0.071	0.063	1.095	0.273	0.03	-0.103	0.072	1.431	0.152	0.15
PCA2	0.096	0.147	0.635	0.526	0.02	-0.311	0.279	1.117	0.264	0.10
TEB	0.222	0.225	0.953	0.341	0.03	0.482	0.329	1.465	0.143	0.19
South America Simpson index_gen										
(Intercept)	4.936	0.027	178.797	0.000	NA	4.841	0.112	43.246	0.000	NA
C:N ratio	0.051	0.024	2.097	0.036	0.79	0.007	0.018	0.386	0.700	0.25
CWD	0.168	0.029	5.802	0.000	1.00	0.102	0.034	3.011	0.003	0.98
Simpson index_gen	-0.045	0.024	1.857	0.063	0.67	-0.013	0.018	0.736	0.462	0.30
MAP	-0.014	0.034	0.397	0.692	0.25	0.008	0.034	0.236	0.813	0.29
MAT	0.023	0.025	0.897	0.370	0.34	-0.010	0.022	0.486	0.627	0.26
PCA1	0.081	0.025	3.249	0.001	1.00	0.000	0.020	0.019	0.985	0.24
PCA2	-0.039	0.018	2.105	0.035	0.80	-0.025	0.017	1.454	0.146	0.48
TEB	-0.006	0.020	0.280	0.780	0.25	0.033	0.015	2.176	0.030	0.78
Africa Simpson index_gen										
(Intercept)	5.188	0.030	170.405	0.000	NA	5.176	0.059	87.222	0.000	NA
C:N ratio	-0.020	0.038	0.512	0.609	0.29	-0.042	0.044	0.956	0.339	0.35
CWD	0.063	0.028	2.240	0.025	0.82	0.100	0.031	3.224	0.001	1.00
Simpson index_gen	-0.019	0.025	0.733	0.464	0.30	-0.035	0.024	1.484	0.138	0.50
MAP	0.064	0.047	1.352	0.176	0.50	-0.032	0.046	0.687	0.492	0.28
MAT	-0.031	0.026	1.186	0.236	0.41	0.034	0.028	1.205	0.228	0.39
PCA1	0.029	0.030	0.953	0.341	0.35	0.040	0.035	1.144	0.252	0.39
PCA2	-0.005	0.039	0.123	0.902	0.25	-0.033	0.043	0.767	0.443	0.30
TEB	-0.070	0.047	1.471	0.141	0.55	-0.013	0.046	0.285	0.776	0.24
Asia Simpson index_gen										
(Intercept)	5.093	0.062	79.113	0.000	NA	5.223	0.144	36.344	0.000	NA
C:N ratio	0.015	0.024	0.598	0.550	0.11	-0.009	0.020	0.444	0.657	0.08
Simpson index_gen	0.046	0.052	0.866	0.387	0.15	0.037	0.040	0.925	0.355	0.12

MAP	0.175	0.041	4.101	0.000	1.00	0.081	0.036	2.261	0.024	0.49
MAT	-0.111	0.055	1.960	0.050	0.61	-0.103	0.041	2.534	0.011	0.71
PCA1	-0.021	0.069	0.290	0.772	0.10	-0.107	0.081	1.316	0.188	0.23
PCA2	0.022	0.150	0.141	0.888	0.08	-0.352	0.251	1.402	0.161	0.27
TEB	0.180	0.235	0.741	0.459	0.12	0.561	0.341	1.646	0.100	0.38
South America Simpson index_fam										
(Intercept)	4.940	0.027	184.100	0.000	NA	4.842	0.111	43.608	0.000	NA
C:N ratio	0.034	0.025	1.386	0.166	0.48	0.006	0.018	0.323	0.747	0.25
CWD	0.166	0.027	6.141	0.000	1.00	0.101	0.034	2.965	0.003	0.98
Simpson index_fam	-0.085	0.028	3.036	0.002	1.00	-0.022	0.021	1.072	0.284	0.37
MAP	-0.011	0.033	0.324	0.746	0.25	0.009	0.034	0.266	0.790	0.29
MAT	0.008	0.025	0.318	0.751	0.25	-0.013	0.022	0.586	0.558	0.27
PCA1	0.064	0.024	2.608	0.009	0.94	-0.001	0.020	0.057	0.955	0.24
PCA2	-0.044	0.018	2.451	0.014	0.90	-0.025	0.017	1.429	0.153	0.47
TEB	-0.003	0.020	0.147	0.883	0.25	0.033	0.015	2.174	0.030	0.78
Africa Simpson index_fam										
(Intercept)	5.189	0.030	171.774	0.000	NA	5.174	0.060	86.253	0.000	NA
C:N ratio	-0.018	0.038	0.472	0.637	0.28	-0.047	0.045	1.024	0.306	0.36
CWD	0.062	0.028	2.233	0.026	0.82	0.100	0.031	3.248	0.001	1.00
Simpson index_fam	-0.017	0.022	0.750	0.453	0.30	-0.034	0.021	1.618	0.106	0.56
MAP	0.065	0.047	1.375	0.169	0.51	-0.026	0.047	0.549	0.583	0.26
MAT	-0.031	0.026	1.190	0.234	0.41	0.031	0.028	1.076	0.282	0.36
PCA1	0.030	0.030	0.974	0.330	0.36	0.047	0.037	1.269	0.204	0.44
PCA2	-0.005	0.039	0.117	0.907	0.25	-0.029	0.044	0.660	0.510	0.28
TEB	-0.069	0.047	1.467	0.142	0.55	-0.011	0.046	0.244	0.808	0.24
Asia Simpson index_fam										
(Intercept)	5.094	0.064	77.731	0.000	NA	5.221	0.144	36.161	0.000	NA
C:N ratio	0.014	0.024	0.578	0.563	0.12	-0.010	0.021	0.481	0.631	0.08
Simpson index_fam	-0.004	0.039	0.086	0.931	0.09	0.025	0.030	0.830	0.407	0.13
MAP	0.176	0.041	4.121	0.000	1.00	0.081	0.036	2.239	0.025	0.48
MAT	-0.110	0.055	1.945	0.052	0.60	-0.102	0.041	2.475	0.013	0.69
PCA1	-0.019	0.069	0.272	0.785	0.10	-0.106	0.081	1.308	0.191	0.23
PCA2	0.010	0.163	0.058	0.954	0.10	-0.352	0.251	1.401	0.161	0.27
TEB	0.189	0.246	0.745	0.456	0.14	0.556	0.341	1.628	0.103	0.39

793

794

795

796

797

798

799

800

801

49

802 **Supplementary Table 6**. Averaged simultaneous autoregressive model coefficients for ln(carbon) in
803 1 ha plots as a function of the community weighted mean of wood density (WD CWM), species
804 richness, climate and soil variables.

Variable	β	SE	Z	P	$\sum \omega_i$
		South America			
Intercept	5.64	0.05	112.06	<0.001	NA
MAT	-0.10	0.03	3.86	<0.001	1
CWD	0.10	0.04	2.67	0.008	0.97
MAP	0.08	0.03	2.61	0.009	0.87
WD CWM	0.15	0.02	6.55	<0.001	0.45
Species richness	0.02	0.02	0.64	0.520	0.43
TEB	0.02	0.02	1.23	0.220	0.4
PCA1	0.01	0.02	0.36	0.721	0.29
C:N	0.00	0.02	0.07	0.941	0.25
PCA2	0.01	0.02	0.40	0.693	0.24
		Africa			
Intercept	5.90	0.06	101.31	<0.001	NA
WD CWM	0.18	0.02	7.61	<0.001	1
MAT	-0.03	0.03	1.37	0.172	1
CWD	0.08	0.03	2.79	0.005	0.96
TEB	0.07	0.03	2.41	0.016	0.92
MAP	-0.05	0.04	1.21	0.228	0.42
Species richness	0.06	0.05	1.29	0.198	0.28
PCA1	-0.02	0.03	0.72	0.469	0.25
PCA2	0.01	0.03	0.20	0.839	0.25
C:N	0.00	0.04	0.08	0.935	0.23
		Asia			
Intercept	5.98	0.11	52.26	<0.001	NA
MAP	0.11	0.03	3.35	0.001	0.99
MAT	-0.13	0.04	3.06	0.002	0.96
Species richness	0.11	0.04	2.50	0.012	0.79
WD CWM	0.17	0.07	2.24	0.025	0.65
C:N	-0.03	0.04	0.79	0.431	0.23
TEB	-0.04	0.07	0.66	0.510	0.2
PCA1	-0.03	0.05	0.59	0.554	0.2
PCA2	-0.03	0.07	0.38	0.707	0.18

805

806

807

808

809

810 **Supplementary Table 7.** Relationship between diversity and carbon in 0.04ha subplots within 1ha
811 forest inventory plots. For each diversity metric, we constructed mixed effects models of ln (carbon)
812 as a function of ln (diversity metric) and ln (stem density) with plot identify as a random effect.
813 Coefficients were assumed to vary between plots, with SD showing the estimated standard deviation
814 of this variation. The effect of doubling a diversity metric on carbon storage was calculated as $(2^\beta - 1)$
815 x 100. ^0D is species richness, ^1D is Shannon diversity and ^2D is Simpson diversity (see SI methods).

Diversity metric	$\beta \pm SE$	SD	Effect of doubling (%)
^0D (species level)	0.096 ± 0.048	0.440	6.9
^0D (genus level)	0.110 ± 0.046	0.432	7.9
^0D (family level)	0.010 ± 0.039	0.338	0.7
^1D (species level)	0.053 ± 0.035	0.324	3.7
^1D (genus level)	0.061 ± 0.035	0.331	4.3
^1D (family level)	-0.007 ± 0.033	0.300	-0.5
^2D (species level)	0.026 ± 0.028	0.262	1.8
^2D (genus level)	0.034 ± 0.028	0.267	2.4
^2D (family level)	-0.020 ± 0.028	0.260	-1.4
^0D (species level) / 10 stems	0.133 ± 0.069	0.585	9.7
^0D (genus level) / 10 stems	0.133 ± 0.064	0.572	9.7
^0D (family level) / 10 stems	0.017 ± 0.011	0.046	1.2

816
817
818
819
820
821
822
823
824
825
826
827
828
829
830

References

831

832 1 Lopez-Gonzalez, G., Lewis, S. L., Burkitt, M. & Phillips, O. L. ForestPlots.net: a web application
833 and research tool to manage and analyse tropical forest plot data. *Journal of Vegetation*
834 *Science* **22**, 610-613, doi:10.1111/j.1654-1103.2011.01312.x (2011).

835 2 Phillips, O. L., Baker, T. R., Feldpausch, T. R. & Brienen, R. J. W. RAINFOR field manual for plot
836 establishment and remeasurement. (University of Leeds, Leeds, 2009).

837 3 IUSS Working GROUP WRB. World reference base for soil resources 2006. (Rome, 2006).

838 4 Quesada, C. A. *et al.* Variations in chemical and physical properties of Amazon forest soils in
839 relation to their genesis. *Biogeosciences* **7**, 1515-1541, doi:10.5194/bg-7-1515-2010 (2010).

840 5 Lewis, S. L. *et al.* Above-ground biomass and structure of 260 African tropical forests.
841 *Philosophical Transactions of the Royal Society B: Biological Sciences* **368**,
842 doi:10.1098/rstb.2012.0295 (2013).

843 6 FAO/ IIASA/ ISRIC/ ISSCAS/ JRC. Harmonized World Soil Database (version 1.2). (Rome, Italy
844 and Laxenburg, Austria, 2012).

845 7 Batjes, J. & through ISRIC/WDC-Soils.   (ed University of Ghent) (Ghent, Belgium, 2007).

846 8 Hijmans, R. J., Cameron, S. E., Parra, J. L., Jones, P. G. & Jarvis, A. Very high resolution
847 interpolated climate surfaces for global land areas. *International Journal of Climatology* **25**,
848 1965-1978, doi:10.1002/joc.1276 (2005).

849 9 Harris, I., Jones, P. D., Osborn, T. J. & Lister, D. H. Updated high-resolution grids of monthly
850 climatic observations – the CRU TS3.10 Dataset. *International Journal of Climatology* **34**, 623-
851 642, doi:10.1002/joc.3711 (2014).

852 10 Vásquez, R. *et al. Flórula de las reservas biológicas de Iquitos, Perú: Allpahuayo-Mishana,*
853 *Explornapo Camp, Explorama Lodge*. (Missouri Botanical Garden, 1997).

854 11 Hill, M. O. Diversity and Evenness: A Unifying Notation and Its Consequences. *Ecology* **54**,
855 427-432, doi:10.2307/1934352 (1973).

856 12 Millar, R. B., Anderson, M. J. & Tolimieri, N. Much ado about nothings: using zero similarity
857 points in distance-decay curves. *Ecology* **92**, 1717-1722, doi:10.1890/11-0029.1 (2011).

858 13 Slik, J. W. F. *et al.* An estimate of the number of tropical tree species. *Proceedings of the*
859 *National Academy of Sciences*, doi:10.1073/pnas.1423147112 (2015).

860 14 Beck, J., Holloway, J. D. & Schwanghart, W. Undersampling and the measurement of beta
861 diversity. *Methods in Ecology and Evolution* **4**, 370-382, doi:10.1111/2041-210x.12023
862 (2013).

863 15 Cayuela, L., Granzow-de la Cerda, Í., Albuquerque, F. S. & Golicher, D. J. taxonstand: An r
864 package for species names standardisation in vegetation databases. *Methods in Ecology and*
865 *Evolution* **3**, 1078-1083, doi:10.1111/j.2041-210X.2012.00232.x (2012).

866 16 Hothorn, T., Bretz, F. & Westfall, P. Simultaneous Inference in General Parametric Models.
867 *Biometrical Journal* **50**, 346-363, doi:10.1002/bimj.200810425 (2008).

868 17 pwr: Basic functions for power analysis. R package version 1.1.1. htto://CRAN.R-
869 project.org/package=pwr (2012).

870 18 Gilpin, A. R. Table for Conversion of Kendall'S Tau to Spearman'S Rho Within the Context of
871 Measures of Magnitude of Effect for Meta-Analysis. *Educational and Psychological*
872 *Measurement* **53**, 87-92, doi:10.1177/0013164493053001007 (1993).

873 19 Barton, K.   (2015).

874 20 ncf: spatial nonparametric covariance functions. R package version 1.1-5. http://CRAN.R-
875 project.org/package=ncf (2013).

876 21 spdep: Spatial dependence: weighting schemes, statsitics and models. R package version 0.5-
877 77. http://CRAN.R-project.org/package=spdep (2014).

878 22 F. Dormann, C. *et al.* Methods to account for spatial autocorrelation in the analysis of
879 species distributional data: a review. *Ecography* **30**, 609-628, doi:10.1111/j.2007.0906-
880 7590.05171.x (2007).

52

881 23 Kissling, W. D. & Carl, G. Spatial autocorrelation and the selection of simultaneous
882   autoregressive models. *Global Ecology and Biogeography* **17**, 59-71, doi:10.1111/j.1466-
883   8238.2007.00334.x (2008).
884 24 Mauricio Bini, L. *et al.* Coefficient shifts in geographical ecology: an empirical evaluation of
885   spatial and non-spatial regression. *Ecography* **32**, 193-204, doi:10.1111/j.1600-
886   0587.2009.05717.x (2009).
887 25 Chisholm, R. A. *et al.* Scale-dependent relationships between tree species richness and
888   ecosystem function in forests. *Journal of Ecology* **101**, 1214-1224, doi:10.1111/1365-
889   2745.12132 (2013).
890 26 lme4: Linear mixed-effects models using Eigen and S4 v. R package version 1.1-7 (2014).
891 27 Loreau, M. & Hector, A. Partitioning selection and complementarity in biodiversity
892   experiments. *Nature* **412**, 72-76, doi:10.1038/35083573 (2001).
893 28 Jucker, T., Bouriaud, O. & Coomes, D. A. Crown plasticity enables trees to optimize canopy
894   packing in mixed-species forests. *Functional Ecology* **29**, 1078-1086, doi:10.1111/1365-
895   2435.12428 (2015).
896 29 Cavanaugh, K. C. *et al.* Carbon storage in tropical forests correlates with taxonomic diversity
897   and functional dominance on a global scale. *Global Ecology and Biogeography* **23**, 563-573,
898   doi:10.1111/geb.12143 (2014).
899 30 Finegan, B. *et al.* Does functional trait diversity predict above-ground biomass and
900   productivity of tropical forests? Testing three alternative hypotheses. *Journal of Ecology* **103**,
901   191-201, doi:10.1111/1365-2745.12346 (2015).
902 31 Zanne, A. E. *et al.* (Dryad Data Repository, 2009).
903 32 Chave, J. *et al.* Towards a worldwide wood economics spectrum. *Ecology Letters* **12**, 351-
904   366, doi:10.1111/j.1461-0248.2009.01285.x (2009).
905 33 Lewis, S. L. *et al.* Increasing carbon storage in intact African tropical forests. *Nature* **457**,
906   1003-1006,
907   doi:http://www.nature.com/nature/journal/v457/n7232/suppinfo/nature07771_S1.html
908   (2009).
909 34 Brienen, R. J. W. *et al.* Long-term decline of the Amazon carbon sink. *Nature* **519**, 344-348,
910   doi:10.1038/nature14283

911 http://www.nature.com/nature/journal/v519/n7543/abs/nature14283.html#supplementary-
912   information (2015).
913 35 Chave, J. *et al.* Assessing Evidence for a Pervasive Alteration in Tropical Tree Communities.
914   *PLoS Biol* **6**, e45, doi:10.1371/journal.pbio.0060045 (2008).
915 36 Baraloto, C. *et al.* Functional trait variation and sampling strategies in species-rich plant
916   communities. *Functional Ecology* **24**, 208-216, doi:10.1111/j.1365-2435.2009.01600.x
917   (2010).
918 37 Wright, S. J. *et al.* Functional traits and the growth‑mortality trade-off in tropical trees.
919   *Ecology* **91**, 3664-3674, doi:10.1890/09-2335.1 (2010).
920 38 Van Gelder, H. A., Poorter, L. & Sterck, F. J. Wood mechanics, allometry, and life-history
921   variation in a tropical rain forest tree community. *New Phytologist* **171**, 367-378,
922   doi:10.1111/j.1469-8137.2006.01757.x (2006).
923 39 Falster, D. S. Sapling strength and safety: the importance of wood density in tropical forests.
924   *New Phytologist* **171**, 237-239, doi:10.1111/j.1469-8137.2006.01809.x (2006).
925 40 Fyllas, N. M., Quesada, C. A. & Lloyd, J. Deriving Plant Functional Types for Amazonian
926   forests for use in vegetation dynamics models. *Perspectives in Plant Ecology, Evolution and*
927   *Systematics* **14**, 97-110, doi:http://dx.doi.org/10.1016/j.ppees.2011.11.001 (2012).
928 41 Aubry-Kientz, M., Hérault, B., Ayotte-Trépanier, C., Baraloto, C. & Rossi, V. Toward Trait-
929   Based Mortality Models for Tropical Forests. *PLoS ONE* **8**, e63678,
930   doi:10.1371/journal.pone.0063678 (2013).

53

931   42   Galbraith, D. *et al.* Residence times of woody biomass in tropical forests. *Plant Ecology &*
932   *Diversity* **6**, 139-157, doi:10.1080/17550874.2013.770578 (2013).
933   43   Petchey, O. L. & Gaston, K. J. Functional diversity: back to basics and looking forward.
934   *Ecology Letters* **9**, 741-758, doi:10.1111/j.1461-0248.2006.00924.x (2006).
935   44   Fauset, S. *et al.* Hyperdominance in Amazonian forest carbon cycling. *Nat Commun* **6**,
936   doi:10.1038/ncomms7857 (2015).
937   45   Slik, J. W. F. *et al.* Large trees drive forest aboveground biomass variation in moist lowland
938   forests across the tropics. *Global Ecology and Biogeography* **22**, 1261-1271,
939   doi:10.1111/geb.12092 (2013).
940   46   Grime, J. P. Benefits of plant diversity to ecosystems: immediate, filter and founder effects.
941   *Journal of Ecology* **86**, 902-910, doi:10.1046/j.1365-2745.1998.00306.x (1998).
942   47   Kraft, N. J. B. *et al.* Disentangling the Drivers of β Diversity Along Latitudinal and Elevational
943   Gradients. *Science* **333**, 1755-1758, doi:10.1126/science.1208584 (2011).

944

945

54